Chapter 2

Theory

This chapter highlights theoretical concepts that are relevant to the quantum chemical and quantum dynamic investigations presented in this thesis. The time-independent Schrödinger equation will be introduced in Section 2.1, after which the electronic and nuclear Schrödinger equations will be treated separately, within the Born-Oppenheimer approximation. In Section 2.2, solutions to the electronic (Section 2.2.1) and nuclear (Section 2.2.2) Schrödinger equations will be presented. The former will involve an overview of common approaches in the field of *ab initio* quantum chemistry, and the latter will focus on numerical methods used to calculate nuclear wave functions and corresponding energies. The time-dependent nuclear Schrödinger equation (TDSE) is reviewed in Section 2.3, including a discussion of numerical methods for solving the TDSE. Finally, angular momentum in quantum mechanics will be reviewed in Section 2.4, focusing on the application of orienting a rigid rotor with the help of an external electric field.

2.1 The time-independent Schrödinger equation

In the absence of spin-orbit coupling, and neglecting other relativistic interactions, the time-independent Schrödinger equation is given as,

$$\hat{\mathbf{H}}|\Phi_{tot}\rangle = \mathcal{E}_{tot}|\Phi_{tot}\rangle \tag{2.1}$$

where $\mathcal{E}_{tot}$ is the total energy, and $|\Phi_{tot}\rangle$ is the total wave function. The molecular Hamiltonian for N electrons and M nuclei is

$$\hat{\mathbf{H}} = \underbrace{-\frac{\hbar^2}{2m_e}\sum_{i=1}^{N}\nabla_i^2 - \frac{\hbar^2}{2}\sum_{A=1}^{M}\frac{1}{m_A}\nabla_A^2}_{\hat{\mathbf{T}}}$$

$$\underbrace{+\left(\sum_{A=1}^{M}\sum_{B>A}^{M}\frac{Z_A Z_B e^2}{4\pi\epsilon_0 R_{AB}} + \sum_{i}^{N}\sum_{j>i}^{N}\frac{e^2}{4\pi\epsilon_0 r_{ij}} - \sum_{i}^{N}\sum_{A}^{M}\frac{Z_A e^2}{4\pi\epsilon_0 r_{iA}}\right)}_{\hat{\mathbf{V}}}. \tag{2.2}$$

Z_A is the atomic number of nucleus A and $-e$ is the charge of the electron. $R_{AB} = |\vec{R}_{AB}|$ is the distance between the Ath and Bth nucleus, $r_{iA} = |\vec{r}_{iA}|$ is distance between the ith electron and Ath nucleus, and the distance between the ith and jth electrons is r_{ij}. The first two terms in Eq. (2.2) compose the operator for the kinetic energy, $\hat{\mathbf{T}}$; the potential energy operator, $\hat{\mathbf{V}}$, is comprised of repulsive and attractive terms. As the separation between the charged electrons and nuclei goes to infinity ($R_{AB} \to \infty$, $r_{iA} \to \infty$, $r_{ij} \to \infty$), these three potential energy terms go to zero, corresponding to the zero level of potential energy.

2.1.1 Born-Oppenheimer approximation

The Schrödinger equation (Eq. 2.1) cannot be solved exactly for systems larger than $H_2{}^+$. To circumvent this problem, one solves the equation by separating electronic and nuclear motion. Due to the significant difference in mass between an electron ($m_e \sim 10^{-31}\,\mathrm{kg}$) and nucleus ($m_{nuc} \sim 10^{-27}\,\mathrm{kg}$), the nuclei can be considered stationary on the time scale of electronic motion. This approximation of separating electronic and nuclear motion is known as the Born-Oppenheimer approximation [98] and holds in general if $(m_e/m_{nuc})^{1/4} \ll 1$. The Born-Oppenheimer approximation thus allows us to solve the electronic and nuclear problems discretely. We will now proceed to consider these two problems separately.

2.1.2 Electronic Schrödinger equation

In order to solve the electronic Schrödinger equation within the Born-Oppenheimer approximation [98], the nuclei are considered fixed on the time scale of electronic motion. One is then able to neglect the nuclear kinetic energy term from Eq. (2.2) and consider

the nuclear repulsion constant. The remaining terms of the Hamiltonian in Eq. (2.2) form the exclusively electronic Hamiltonian, which can be written as [99],

$$\hat{\mathbf{H}}_{el} = -\frac{\hbar^2}{2m_e}\sum_{i=1}^{N}\nabla_i^2 - \sum_{i}^{N}\sum_{A}^{M}\frac{Z_A e^2}{4\pi\epsilon_0 r_{iA}} + \sum_{i}^{N}\sum_{j>i}^{N}\frac{e^2}{4\pi\epsilon_0 r_{ij}}. \tag{2.3}$$

The electronic Schrödinger equation is then just

$$\hat{\mathbf{H}}_{el}\Phi_{el} = \mathcal{E}_{el}\Phi_{el}, \tag{2.4}$$

where $\mathcal{E}_{el}$ is the electronic energy and Φ_{el} is the electronic wave function,

$$\Phi_{el} = \Phi_{el}\left(\{\vec{r}_i\};\{\vec{R}_A\}\right) \tag{2.5}$$

which depend explicitly on the electronic coordinates $\{\vec{r}_i\}$ but parametrically on the nuclear coordinates $\{\vec{R}_A\}$. The total energy for fixed nuclei, also known as the potential energy for a given electronic state, $\hat{\mathbf{V}}_{el}\left(\{\vec{R}_A\}\right)$, consists of the electronic energy $\mathcal{E}_{el}$ and a constant nuclear repulsion term:

$$\hat{\mathbf{V}}_{el}\left(\{\vec{R}_A\}\right) = \mathcal{E}^{el}_{tot}\left(\{\vec{R}_A\}\right) = \mathcal{E}_{el}\left(\{\vec{R}_A\}\right) + \sum_{A=1}^{M}\sum_{B>A}^{M}\frac{Z_A Z_B e^2}{4\pi\epsilon_0 R_{AB}}. \tag{2.6}$$

The notation $\mathcal{E}^{el}_{tot}$ emphasizes that the total energy, in general, depends on the electronic state of the system.

2.1.3 Nuclear Schrödinger equation

In the same manner in which the electronic problem was solved, the nuclear portion of the Schrödinger equation can be solved by invoking the Born-Oppenheimer approximation. Since the electrons move much faster than the nuclei, the electronic coordinates can be replaced by values obtained by averaging over the electronic wave function. In this effective electronic field, the nuclear Hamiltonian can be expressed [99]:

$$\hat{\mathbf{H}}^{el}_{nuc} = -\frac{\hbar^2}{2}\sum_{A=1}^{M}\frac{1}{m_A}\nabla_A^2 + \underbrace{\mathcal{E}_{el}\left(\{\vec{R}_A\}\right) + \sum_{A=1}^{M}\sum_{B>A}^{M}\frac{Z_A Z_B e^2}{4\pi\epsilon_0 R_{AB}}}_{\hat{\mathbf{v}}_{el}\left(\{\vec{R}_A\}\right)}. \tag{2.7}$$

The solutions to the nuclear Schrödinger equation for a given electronic state,

$$\hat{\mathbf{H}}^{el}_{nuc}\Phi^{el}_{nuc} = \mathcal{E}^{el}_{nuc}\Phi^{el}_{nuc} \tag{2.8}$$

are the set of nuclear wave functions Φ^{el}_{nuc} that depend on the nuclear coordinates $\{\vec{R}_A\}$, and in general, on time:

$$\Phi^{el}_{nuc} = \Phi^{el}_{nuc}\left(\{\vec{R}_A\};t\right) \tag{2.9}$$

and $\mathcal{E}_{nuc}^{el}$ is now the total energy in the Born-Oppenheimer approximation ($\equiv\mathcal{E}_{tot}$ from Eq. (2.1)) and contains electronic, translational, vibrational, and rotational energy. The total time-dependent wave function within the Born-Oppenheimer approximation is then the product of the electronic and nuclear wave functions, in which the electronic wave function is considered time-independent and the nuclear wave function is explicitly time-dependent:

$$\Phi_{tot}\left(\{\vec{r}_i\};\{\vec{R}_A\};t\right) = \Phi_{el}\left(\{\vec{r}_i\};\{\vec{R}_A\}\right)\Phi_{nuc}^{el}\left(\{\vec{R}_A\};t\right). \tag{2.10}$$

For stationary states, the time-dependence of the nuclear wave packet is explicitly given as

$$\Phi_{nuc}^{el}\left(\{\vec{R}_A\};t\right) = \tilde{\Phi}_{nuc}^{el}\left(\{\vec{R}_A\}\right)\cdot e^{-E_{nuc}^{el}t/\hbar}, \tag{2.11}$$

with nuclear eigenstates $\tilde{\Phi}_{nuc}^{el}\left(\{\vec{R}_A\}\right)$ and eigenenergies E_{nuc}^{el}. Later, in Chapter 3, these eigenstates will be calculated for the systems FHF^- and OHF^-, and the notation "˜" will be dropped for simplicity. In Chapter 4, we shall consider the time evolution of non-stationary wave packets.

The nuclear wave functions $\Phi_{nuc}^{el}\left(\{\vec{R}_A\};t\right)$ depend on the electronic state, as denoted by the superscript *el*. In the remainder of this thesis, however, only the electronic ground state will be considered, *i.e.* $el=0$, so the superscript will be dropped for the sake of simplicity.

2.2 Solving the Schrödinger equation

We now turn our attention to methods used for solving the electronic (Eq. (2.4)) and nuclear (Eq. (2.8)) Schrödinger equations. Reviewing Eq. (2.7), one sees that the energy obtained by solving the electronic problem provides a potential energy for nuclear motion. Thus, solving the electronic problem will naturally provide us with the framework within which to solve the nuclear Schrödinger equation. Accordingly, we will review the electronic problem first, limiting the discussion to methods that are germane to this work.

2.2.1 Solutions to the electronic problem

Hartree-Fock

Recall the problem we are interested in, Eq. (2.4). The electronic Hamiltonian, $\hat{\mathbf{H}}_{el}$, can be solved exactly for hydrogen, and very accurate wave functions have been calculated for helium and lithium. For atoms containing many electrons, however, obtaining highly accurate wave functions is nontrivial. Calculations often rely on the Hartree-Fock method in which an approximate antisymmetric wave function—or Slater determinant—is constructed from one-electron functions and then optimized [99]. For an N-electron system, this determinant is given as:

$$|\Psi_0\rangle = \frac{1}{\sqrt{N!}} \begin{vmatrix} \chi_1(\vec{x}_1) & \chi_2(\vec{x}_1) & \cdots & \chi_N(\vec{x}_1) \\ \chi_1(\vec{x}_2) & \chi_2(\vec{x}_2) & \cdots & \chi_N(\vec{x}_2) \\ \cdots & \cdots & \cdots & \cdots \\ \chi_1(\vec{x}_N) & \chi_2(\vec{x}_N) & \cdots & \chi_N(\vec{x}_N) \end{vmatrix}. \tag{2.12}$$

The notation $|\Psi_0\rangle$ is used now to distinguish the approximate wave function from the exact electronic wave function $|\Phi_{el}\rangle$ from Eq. (2.5). The rows of the determinant are labelled by electrons, and the columns are labelled by orbitals. The factor $(N!)^{-1/2}$ is a normalization factor and $\chi_i(\vec{x}_i)$ represent occupied spin orbitals that are constrained to be orthonormal,

$$\langle \chi_i | \chi_j \rangle = \delta_{ij}. \tag{2.13}$$

These spin orbitals have the form

$$\chi(\vec{x}) = \begin{cases} \psi(\vec{r})\alpha(\varpi) \\ \text{ or} \\ \psi(\vec{r})\beta(\varpi) \end{cases} \tag{2.14}$$

where $\vec{x}$ is a coordinate that includes spatial ($\vec{r}$) and spin (ϖ) coordinates [99]. The spatial orbital $\psi(\vec{r})$ is a function of the position vector $\vec{r}$; the orthonormal spin functions

$\alpha(\varpi)$ and $\beta(\varpi)$, correspond to spin up ($\uparrow$) and spin down ($\downarrow$). In general, given a set of K spatial orbitals, $\{\psi_i | i = 1, 2, \ldots, K\}$, one can form a set of $2K$ spin orbitals, $\{\chi_i | i = 1, 2, \ldots, 2K\}$.

The single determinant of Eq. (2.12), written in shorthand with just the diagonal elements and including the normalization constant, $|\Psi_0\rangle = |\chi_1 \chi_2 \cdots \chi_N\rangle$, is the simplest possible antisymmetric wave function to describe an electronic state of N electrons, *e.g.* the ground state. The *variation principle*, applied to this single antisymmetric wave function, states that the best determinant is that which gives the lowest Hartree-Fock electronic energy E_{HF},

$$E_{HF} = \langle \Psi_0 | \hat{\mathbf{H}}_{el} | \Psi_0 \rangle, \tag{2.15}$$

where $|\Psi_0\rangle$ denotes the electronic ground state wave function. The optimization relies on minimizing the electronic energy E_{HF} with respect to the set of single-electron spin orbitals $\chi(\vec{x}_i)$. The eigenvalue problem that can be formulated is [99]:

$$\hat{\mathbf{f}}(\vec{x}_i)\chi(\vec{x}_i) = \varepsilon_i \chi(\vec{x}_i), \tag{2.16}$$

where ε_i is the energy of the ith orbital. Eq. (2.16) is referred to as the Hartree-Fock equation and $\hat{\mathbf{f}}(\vec{x}_i)$ is an effective one-electron operator, called the Fock operator, which has the form,

$$\hat{\mathbf{f}}(\vec{x}_i) = \underbrace{-\frac{\hbar^2}{2m_e}\nabla_i^2 - \sum_{A=1}^{M} \frac{Z_A e^2}{4\pi\epsilon_0 r_{iA}}}_{\hat{\mathbf{h}}(\vec{x}_i)} + \mathrm{V}^{HF}(\vec{x}_i). \tag{2.17}$$

The first and second terms in Eq. (2.17) compose the one-electron *core* Hamiltonian, $\hat{\mathbf{h}}(\vec{x}_i)$ for the ith electron, where the first term is just the kinetic energy of the ith electron, and the second term is the potential energy for the attraction between the ith electron and each of the nuclei. $\mathrm{V}^{HF}(\vec{x}_i)$ is the so-called effective Hartree-Fock potential which accounts for two-electron potential energies and is calculated as an average potential experienced by the ith electron in the environment of the other $N-1$ electrons. The Fock operator can be rewritten to express $\mathrm{V}^{HF}(\vec{x}_i)$ explicitly as the total averaged potential arising from one-electron coulomb and exchange potentials. For instance, for electron 1, $\hat{\mathbf{f}}(\vec{x}_1)$ is written as,

$$\hat{\mathbf{f}}(\vec{x}_1) = \hat{\mathbf{h}}(\vec{x}_1) + \sum_{b}^{N} \hat{\mathbf{J}}_b(\vec{x}_1) - \sum_{b}^{N} \hat{\mathbf{K}}_b(\vec{x}_1). \tag{2.18}$$

$\hat{\mathbf{J}}_b(\vec{x}_1)$ and $\hat{\mathbf{K}}_b(\vec{x}_1)$ are the one-electron coulomb and exchange operators, respectively, and they are defined by

$$\hat{\mathbf{J}}_b(\vec{x}_1)\chi_a(\vec{x}_1) = \left[\int d\vec{x}_2 \, \chi_b^*(\vec{x}_2) \frac{1}{\hat{\mathbf{r}}_{12}} \chi_b(\vec{x}_2)\right] \chi_a(\vec{x}_1) \tag{2.19}$$

$$\hat{\mathbf{K}}_b(\vec{x}_1)\chi_a(\vec{x}_1) = \left[\int d\vec{x}_2 \chi_b^*(\vec{x}_2) \frac{1}{\hat{\mathbf{r}}_{12}} \chi_a(\vec{x}_2)\right] \chi_b(\vec{x}_1). \tag{2.20}$$

Here, the indices a and b refer to the occupied spin orbitals of electrons 1 and 2, respectively. The two-electron potential operator $\hat{\mathbf{r}}_{12}^{-1}$ describes the interaction of electron 1 with electron 2; integration over all space and spin coordinates of electron 2, $\vec{x}_2$, yields an effective one-electron potential for electron 1. The coulomb operator, $\hat{\mathbf{J}}_b(\vec{x}_1)$, can be interpreted "classically" as the average local repulsion potential that electron 1 feels sitting in the spin orbital χ_a, arising from electron 2 occupying spin orbital χ_b. The exchange operator, $\hat{\mathbf{K}}_b(\vec{x}_1)$, however, has no classical interpretation: operating on $\chi_a(\vec{x}_1)$ leads to an exchange of electron 1 to the spin orbital χ_b. Unlike the coulomb operator, the exchange operator is a nonlocal operator since the energy contribution comes from a delocalized interaction between electron 1 and electron 2. By summing over all electrons $b \neq a$ in Eq. (2.18), one obtains a total averaged potential acting on the electron in χ_a, arising from the $N-1$ electrons in the other spin orbitals.

Returning now to the eigenvalue problem given in Eq. (2.16), one notices that the Fock operator itself depends on its eigenfunctions $\chi(\vec{x}_i)$ (see Eqs. (2.19) and (2.20)), i.e. the energy of the ith electron will depend on the spin orbitals of the other electrons. Eq. (2.16) is thus nonlinear and must be solved iteratively. The procedure consists of the following steps: an initial set of spin orbitals is used to calculate an initial average field, $\mathrm{V}^{HF}(\vec{x}_i)$; the eigenvalue problem is solved and new orbitals are generated and compared with the initial ones. If the numerical convergence criteria are not satisfied, the procedure is repeated iteratively until self-consistency—or a self-consistent field (SCF)—has been reached. The final orthonormal canonical Fock spin orbitals, $\{\chi_i\}$, have energies $\{\varepsilon_i\}$ and these orbitals can be used to construct a Slater determinant which describes the electronic ground state wave function. Now, before discussing these intermediate steps in more detail, let us examine the differences between determinants constructed using doubly-occupied spatial orbitals and those with singly-occupied spatial orbitals.

Restricted and unrestricted Hartree-Fock

Earlier (see Eq. (2.14)), we stated that $2K$ spin orbitals χ_i can be formed from K spatial orbitals, ψ_i, if each spatial orbital is multiplied by either the α or β spin function.

$$\left.\begin{aligned} \chi_{2i-1}(\vec{x}) &= \psi_i(\vec{r})\alpha(\varpi) \\ \chi_{2i}(\vec{x}) &= \psi_i(\vec{r})\beta(\varpi) \end{aligned}\right\} i = 1, 2, \ldots, K \tag{2.21}$$

In Eq. (2.21), we are implying that the set of spatial orbitals needed to describe electrons of α spin are identical to those used to describe electrons of β spin, *i.e.* $\psi_i^\alpha \equiv \psi_i^\beta \equiv \psi_i$. In such a situation, the spin orbitals are said to be *restricted*, and the Hartree-Fock determinant formed from such spin orbitals is also restricted. In an *unrestricted* system,

the spatial functions describing α and β electrons are different, $\psi_i^\alpha \neq \psi_i^\beta$, and therefore,

$$\left.\begin{array}{rl} \chi_{2i-1}(\vec{x}) = & \psi_i^\alpha(\vec{r})\alpha(\varpi) \\ \chi_{2i}(\vec{x}) = & \psi_i^\beta(\vec{r})\beta(\varpi) \end{array}\right\} i = 1, 2, \ldots, K \tag{2.22}$$

In the case of a determinant with an *even* number of electrons, each spatial orbital is doubly occupied,

$$\{\psi_a | a = 1, 2, \ldots, N/2\}, \tag{2.23}$$

where ψ_a refers to occupied spatial orbitals. The system is then said to have a *closed-shell*. If a spatial orbital contains a single electron, the system is referred to as having an *open-shell*. An open-shell system is usually described using unrestricted determinants (unrestricted Hartree-Fock≡UHF) since the energy involving an unpaired α electron is different from that of an unpaired β electron, whereas closed-shell systems are described using a restricted determinant (restricted Hartree-Fock≡RHF). Restricted determinants can, however, also be employed to describe an open-shell system; this case is referred to as restricted open-shell (ROHF). Finally, one should note that in the case of an even number of electrons in an unrestricted determinant, the UHF solution is identical to that of the RHF one.

For clarity, let us first examine the closed-shell, restricted case in more detail, before returning to the unrestricted case. The determinant of the closed-shell restricted ground state is

$$|\Psi_0\rangle = |\chi_1\chi_2\cdots\chi_{N-1}\chi_N\rangle = |\psi_1\bar{\psi}_1\cdots\psi_a\bar{\psi}_a\cdots\psi_{N/2}\bar{\psi}_{N/2}\rangle, \tag{2.24}$$

where the bar denotes spatial orbitals containing electrons with down spin. One can now easily convert the Hartree-Fock equation (Eq. (2.16)) in terms of spin orbitals to an equation in terms of spatial orbitals by integrating out the spin functions,

$$\hat{\mathbf{f}}(\vec{r}_1)\psi_i(\vec{r}_1) = \int d\varpi_1 \alpha^*(\varpi_1)\hat{\mathbf{f}}(\vec{x}_1)\alpha(\varpi_1) = \varepsilon_i\psi_i(\vec{r}_1), \tag{2.25}$$

where the integration in Eq. (2.25) is performed over *e.g.* electron 1 with α spin. A similar integration can be performed over the variables corresponding to β spin. Then, Eq. (2.18) can be rewritten for the closed-shell Fock operator [99],

$$\hat{\mathbf{f}}(\vec{r}_1) = \hat{\mathbf{h}}(\vec{r}_1) + \sum_a^{N/2} 2\hat{\mathbf{J}}_a(\vec{r}_1) - \hat{\mathbf{K}}_a(\vec{r}_1), \tag{2.26}$$

where the closed-shell coulomb and exchange operators are defined by

$$\hat{\mathbf{J}}_a(\vec{r}_1)\psi_i(\vec{r}_1) = \left[\int d\vec{r}_2 \psi_a^*(\vec{r}_2)\frac{1}{\hat{\mathbf{r}}_{12}}\psi_a(\vec{r}_2)\right]\psi_i(\vec{r}_1) \tag{2.27}$$

$$\hat{\mathbf{K}}_a(\vec{r}_1)\psi_i(\vec{r}_1) = \left[\int d\vec{r}_2 \psi_a^*(\vec{r}_2)\frac{1}{\hat{\mathbf{r}}_{12}}\psi_i(\vec{r}_2)\right]\psi_a(\vec{r}_1). \tag{2.28}$$

The closed-shell restricted Hartree-Fock equation is then

$$\hat{\mathbf{f}}(\vec{r}_1)\psi_i(\vec{r}_1) = \varepsilon_i\psi_i(\vec{r}_1), \tag{2.29}$$

with the set of *spatial* orbital energies $\{\varepsilon_i\}$.

Let us return now to unrestricted determinants. Since electrons of α and β spin will have a different number of coulomb and exchange integrals depending on the number of remaining α and β electrons in the determinant, the energies corresponding to electrons of opposite spin will be different. In order to account for these energy differences, spatial functions corresponding to electrons of opposite spin must be different, *i.e.* $\psi_i^\alpha \neq \psi_i^\beta$. We can substitute the unrestricted set of spin orbitals (Eq. (2.22)) into the Hartree-Fock eigenvalue equation and follow the same procedure that was used in the case of a restricted determinant (see Eq. (2.25)). One obtains

$$\hat{\mathbf{f}}^\alpha(\vec{r}_1)\psi_i^\alpha(\vec{r}_1) = \varepsilon_i^\alpha\psi_i^\alpha(\vec{r}_1) \tag{2.30}$$

$$\hat{\mathbf{f}}^\beta(\vec{r}_1)\psi_i^\beta(\vec{r}_1) = \varepsilon_i^\beta\psi_i^\beta(\vec{r}_1), \tag{2.31}$$

where ε_i^α and ε_i^β are the energies of the spatial orbitals ψ_i^α and ψ_i^β, respectively. Eqs. (2.30) and (2.31) are the equations defining the unrestricted spatial orbitals ψ_i^α and ψ_i^β (compare with Eq. (2.29)). The unrestricted, spatial Fock operators $\hat{\mathbf{f}}^\alpha(\vec{r}_1)$ and $\hat{\mathbf{f}}^\beta(\vec{r}_1)$ are given as

$$\hat{\mathbf{f}}^\alpha(\vec{r}_1) = \hat{\mathbf{h}}(\vec{r}_1) + \sum_a^{N^\alpha}\left[J_a^\alpha(\vec{r}_1) - K_a^\alpha(\vec{r}_1)\right] + \sum_a^{N^\beta} J_a^\beta(\vec{r}_1) \tag{2.32}$$

$$\hat{\mathbf{f}}^\beta(\vec{r}_1) = \hat{\mathbf{h}}(\vec{r}_1) + \sum_a^{N^\beta}\left[J_a^\beta(\vec{r}_1) - K_a^\beta(\vec{r}_1)\right] + \sum_a^{N^\alpha} J_a^\alpha(\vec{r}_1), \tag{2.33}$$

where $N^\alpha + N^\beta = N$. The Fock operator $\hat{\mathbf{f}}^\alpha$ for an electron with α spin (Eq. (2.32)), for example, includes kinetic energy, nuclear attraction, and an effective potential of an electron with α spin. One should note that the effective interactions of an electron with α spin include coulomb repulsion energies arising from interactions with all other electrons (with both α and β spin), but an exchange interaction only with electrons of the same (in this case, α) spin.

Having discussed restricted (Eq. (2.29)) and unrestricted (Eqs. (2.30) and (2.31)) Hartree-Fock equations, we now turn our attention to solving these equations, beginning with the restricted case.

The Roothaan-Hall Equations

By introducing a set of known spatial basis functions, Eq. (2.25) can be solved using a set of algebraic equations [100, 101]. In general, this calculation relies on expanding the

set ψ_i as a linear combination of K known basis functions $\{\phi_\mu(\vec{r})|\mu = 1, 2, \ldots, K\}$,

$$\psi_i(\vec{r}_i) = \sum_\mu \mathbf{C}_{\mu i}\phi_\mu(\vec{r}_i) \qquad i = 1, 2, \ldots, K \tag{2.34}$$

where the $\mathbf{C}_{\mu i}$ are expansion coefficients. The set $\{\phi_\mu\}$ is, of course, finite, since for practical computational purposes one must find a compromise between accuracy and efficiency, and the series is truncated. For an infinite set of $\{\phi_\mu\}$, the expansion would be exact. One can now substitute Eq. (2.34) into Eq. (2.29), and using the index ν, obtain

$$\hat{\mathbf{f}}(\vec{r}_1)\sum_\nu \mathbf{C}_{\nu i}\phi_\nu(\vec{r}_1) = \varepsilon_i \sum_\nu \mathbf{C}_{\nu i}\phi_\nu(\vec{r}_1). \tag{2.35}$$

Multiplication with $\phi^*_\mu(1)$ and integration over the coordinates of electron 1 leads to

$$\sum_\nu \mathbf{C}_{\nu i}\int d\vec{r}_1\phi^*_\mu(\vec{r}_1)\,\hat{\mathbf{f}}(\vec{r}_1)\,\phi_\nu(\vec{r}_1) = \varepsilon_i \sum_\nu \mathbf{C}_{\nu i}\int d\vec{r}_1\phi^*_\mu(\vec{r}_1)\phi_\nu(\vec{r}_1). \tag{2.36}$$

At this point, two matrices are generally defined, the overlap matrix $\mathbf{S}$ and the Fock matrix, $\mathbf{F}$. The overlap matrix of dimension $K \times K$ has the elements

$$\mathbf{S}_{\mu\nu} = \int d\vec{r}_1\phi^*_\mu(\vec{r}_1)\phi_\nu(\vec{r}_1) \tag{2.37}$$

and is Hermitian. The basis functions $\{\phi_\mu\}$ are normalized but not necessarily orthogonal, such that they overlap with a magnitude $0 \leq |\mathbf{S}_{\mu\nu}| \leq 1$, where the diagonal elements of $\mathbf{S}$ are 1 and the off-diagonal are less than 1. The Fock matrix is defined as follows:

$$\mathbf{F}_{\mu\nu} = \int d\vec{r}_1\phi^*_\mu(\vec{r}_1)\,\hat{\mathbf{f}}(\vec{r}_1)\,\phi_\nu(\vec{r}_1) \tag{2.38}$$

and is also a $K \times K$ Hermitian matrix. Eq. (2.36) can now be rewritten in terms of the overlap and Fock matrices:

$$\sum_\nu \mathbf{F}_{\mu\nu}\mathbf{C}_{\nu i} = \varepsilon_i \sum_\nu \mathbf{S}_{\mu\nu}\mathbf{C}_{\nu i} \qquad i = 1, 2, \ldots, K, \tag{2.39}$$

where K is the number of spatial basis functions, from which $2K$ spin functions can be constructed. For N electrons, $N/2$ occupied and $K - N/2$ unoccupied, or virtual, spatial orbitals exist. In its most compact form, Eq. (2.36) is written as

$$\mathbf{FC} = \mathbf{SC}\boldsymbol{\varepsilon}. \tag{2.40}$$

Eq. (2.40) is a single matrix equation that describes what are referred to as the *Roothaan-Hall* equations [100, 101], where $\mathbf{C}$ is now a $K \times K$ square matrix

$$\mathbf{C} = \begin{pmatrix} C_{11} & C_{12} & \cdots & C_{1K} \\ C_{21} & C_{22} & \cdots & C_{2K} \\ \vdots & \vdots & & \vdots \\ C_{K1} & C_{K2} & \cdots & C_{KK} \end{pmatrix} \tag{2.41}$$

where the columns correspond to the molecular orbitals. $\boldsymbol{\varepsilon}$ is a diagonal matrix of the (spatial) orbital energies ε_i:

$$\boldsymbol{\varepsilon} = \begin{pmatrix} \varepsilon_1 & & & & & \\ & \varepsilon_2 & & & & 0 \\ & & \ddots & & & \\ & & & \varepsilon_i & & \\ & 0 & & & \ddots & \\ & & & & & \varepsilon_K \end{pmatrix}. \tag{2.42}$$

The Fock matrix $\mathbf{F}$ is the matrix form of the Fock operator (Eq. (2.26)) that consists of the core Hamiltonian and the contributions from two-electron integrals.

The Roothaan-Hall equations therefore allow for the calculation of molecular orbitals from the restricted Hartree-Fock equations. Analogously, the *Pople-Nesbet* equations [102] can be derived for the unrestricted Hartree-Fock equations, and they have the form

$$\mathbf{F}^{\alpha}\mathbf{C}^{\alpha} = \mathbf{S}\mathbf{C}^{\alpha}\boldsymbol{\varepsilon}^{\alpha} \tag{2.43}$$

$$\mathbf{F}^{\beta}\mathbf{C}^{\beta} = \mathbf{S}\mathbf{C}^{\beta}\boldsymbol{\varepsilon}^{\beta}. \tag{2.44}$$

In general, larger and larger basis sets (for a review of basis sets, see *e.g.* Ref. [103]) will lower the Hartree-Fock energy E_{HF}, and in the limit of infinite basis functions ($K \rightarrow \infty$), the *Hartree-Fock limit* is reached,

$$E_{HF} = \langle \Psi_0 | \hat{\mathbf{H}}_{el} | \Psi_0 \rangle. \tag{2.45}$$

In practice, any finite number of basis functions will lead to an energy above the Hartree-Fock limit. The difference between the exact nonrelativistic energy of the electronic ground state (in the Born-Oppenheimer approximation), $\mathcal{E}_0$, and the Hartree-Fock energy, E_{HF}, is what is called the correlation energy,

$$E_{corr} = \mathcal{E}_0 - E_{HF}. \tag{2.46}$$

Since E_{HF} is an upper bound to the exact energy, the correlation energy is negative. Correlation energy arises since the motion of electrons with opposite spin is not correlated within the Hartree-Fock approach. Several quantum chemical methods attempt to recover this correlation energy by improving upon the Hartree-Fock approximation, and in the following, we will examine some of these approaches.

Configuration interaction

In general, for N electrons and $2K$ spin orbitals (K spatial orbitals), multiple electronic configurations exist in which electrons have been excited from occupied spin orbitals, $\chi_a, \chi_b, \ldots$, to virtual spin orbitals, $\chi_r, \chi_s, \ldots$. A wave function describing a single excitation of an electron from χ_a to χ_r would be denoted

$$|\Psi_a^r\rangle = |\chi_1\chi_2\cdots\chi_r\chi_b\cdots\chi_N\rangle, \tag{2.47}$$

and in the case of two excited electrons, χ_a and χ_b to χ_r to χ_s, one would write

$$|\Psi_{ab}^{rs}\rangle = |\chi_1\chi_2\cdots\chi_r\chi_s\cdots\chi_N\rangle, \tag{2.48}$$

and so on, such that the exact electronic wave function for any state of the system within a given basis set can be written as an expansion of all the electronic configurations [99],

$$|\Phi_0\rangle = c_0|\Psi_0\rangle + \sum_{ra} c_a^r|\Psi_a^r\rangle + \sum_{\substack{a<b\\r<s}} c_{ab}^{rs}|\Psi_{ab}^{rs}\rangle + \sum_{\substack{a<b<c\\r<s<t}} c_{abc}^{rst}|\Psi_{abc}^{rst}\rangle + \sum_{\substack{a<b<c<d\\r<s<t<u}} c_{abcd}^{rstu}|\Psi_{abcd}^{rstu}\rangle + \cdots, \tag{2.49}$$

where here we have just considered the exact wave function for the electronic ground state, $|\Phi_0\rangle$. Eq. (2.49) can be written more compactly,

$$|\Phi_0\rangle = c_0|\Psi_0\rangle + c_S|S\rangle + c_D|D\rangle + c_T|T\rangle + c_Q|Q\rangle + \cdots, \tag{2.50}$$

where $|S\rangle$ represents terms involving single excitations, *i.e.* $|\Psi_a^r\rangle$, $|D\rangle$ represents terms involving double excitations, *i.e.* $|\Psi_{ab}^{rs}\rangle$, and so on, with corresponding expansion coefficients, c_S, c_D, c_T, c_Q *etc.*. In general, ground and excited states of an N-electron system can be written as a linear combination of all possible N-electron Slater determinants—or electronic configuration interactions (CI). Accordingly, an infinite set of N-electron determinants constitutes a complete description of the N-electron wave function, and is referred to as "full CI" (FCI). The elements of the FCI matrix are,

	$\|\Psi_0\rangle$	$\|\Psi_a^r\rangle$	$\|\Psi_{ab}^{rs}\rangle$	$\|\Psi_{abc}^{rst}\rangle$	$\|\Psi_{abcd}^{rstu}\rangle$	$\cdots$
	$\|\Psi_0\rangle$	$\|S\rangle$	$\|D\rangle$	$\|T\rangle$	$\|Q\rangle$	$\cdots$
$\|\Psi_0\rangle$	$\langle\Psi_0\|\hat{\mathbf{H}}_{el}\|\Psi_0\rangle$	0	$\langle\Psi_0\|\hat{\mathbf{H}}_{el}\|D\rangle$	0	0	$\cdots$
$\|S\rangle$	0	$\langle S\|\hat{\mathbf{H}}_{el}\|S\rangle$	$\langle S\|\hat{\mathbf{H}}_{el}\|D\rangle$	$\langle S\|\hat{\mathbf{H}}_{el}\|T\rangle$	0	$\cdots$
$\|D\rangle$	$\langle D\|\hat{\mathbf{H}}_{el}\|\Psi_0\rangle$	$\langle D\|\hat{\mathbf{H}}_{el}\|S\rangle$	$\langle D\|\hat{\mathbf{H}}_{el}\|D\rangle$	$\langle D\|\hat{\mathbf{H}}_{el}\|T\rangle$	$\langle D\|\hat{\mathbf{H}}_{el}\|Q\rangle$	$\cdots$
$\|T\rangle$	0	$\langle T\|\hat{\mathbf{H}}_{el}\|S\rangle$	$\langle T\|\hat{\mathbf{H}}_{el}\|D\rangle$	$\langle T\|\hat{\mathbf{H}}_{el}\|T\rangle$	$\langle T\|\hat{\mathbf{H}}_{el}\|Q\rangle$	$\cdots$
$\|Q\rangle$	0	0	$\langle Q\|\hat{\mathbf{H}}_{el}\|D\rangle$	$\langle Q\|\hat{\mathbf{H}}_{el}\|T\rangle$	$\langle T\|\hat{\mathbf{H}}_{el}\|Q\rangle$	$\langle Q\|\hat{\mathbf{H}}_{el}\|Q\rangle\cdots$
$\vdots$	$\vdots$	$\vdots$	$\vdots$	$\vdots$	$\vdots$	$\vdots$

(2.51)

where $|\Psi_0\rangle$ is the determinant formed from the N lowest energy spin orbitals. The eigenvalues of the trial function Eq. (2.49) are obtained by constructing the matrix representation of the Hamiltonian in the basis of the N-electron functions, and then solving for the eigenvalues of the FCI matrix (Eq. (2.51)). Since wave functions with a different *total* spin do not mix, *i.e.* $\langle\Psi_i|\hat{\mathbf{H}}_{el}|\Psi_j\rangle = 0$ if $|\Psi_i\rangle$ and $|\Psi_j\rangle$ have different total spin, several of these determinants can be eliminated from the trial function [99]. From Eq. (2.51), one sees that the evaluation of the integrals $\langle\Psi_i|\hat{\mathbf{H}}_{el}|\Psi_j\rangle$ will involve calculating terms of the type $\langle\Psi_0|\hat{\mathbf{H}}_{el}|\Psi_a^r\rangle$, which involve single excitations, $\langle\Psi_0|\hat{\mathbf{H}}_{el}|\Psi_{ab}^{rs}\rangle$ which involve double excitations, and so on. From all these terms, some can be eliminated. For example, the *Brillouin* theorem states that determinants containing a single excitation $|\Psi_a^r\rangle$ will not interact directly with a reference Hartree-Fock determinant [99], *i.e.*

$$\langle\Psi_0|\hat{\mathbf{H}}_{el}|\Psi_a^r\rangle = 0. \tag{2.52}$$

Instead, contributions from single excitations mix indirectly with $|\Psi_0\rangle$ through the terms corresponding to double excitations, $\langle\Psi_a^r|\hat{\mathbf{H}}_{el}|\Psi_{ab}^{rs}\rangle$ and $\langle\Psi_{ab}^{rs}|\hat{\mathbf{H}}_{el}|\Psi_0\rangle$. Furthermore, for determinants that differ by three or more spin orbitals, the matrix element is zero, $\langle\Psi_0|\hat{\mathbf{H}}_{el}|\Psi_{abc}^{rst}\rangle$=0 [99]. As a result, double excitations mix directly with the ground state determinant and bear the most contribution to the ground state correlation energy. Triple excitations contribute to the ground state energy by mixing with double excitations, as do quadruple excitations. Although single excitations have a small effect on the ground state energy, they play a critical role in the calculation of excited electronic states, as well as in the determination of other molecular properties, such as charge distribution and therefore in the calculation of the dipole moment.

The variation principle implies that the lowest full CI eigenenergy will be an upper bound to the electronic ground state energy. Futhermore, the higher eigenvalues will be upper bounds to the electronic excited state energies [104]. In practice, the full CI matrix becomes computationally unrealistic, except for very small systems. Even for a single-electron basis of moderate size, myriad determinants exist. The common solution is thus to truncate the expansion to include only configurations that differ from the Hartree-Fock ground state by a certain number of spin orbitals. Single (CIS), single/double (CISD), and single/double/triple (CISDT) excitations can be routinely included. One serious drawback of truncated CI energies, however, is their lack of size-consistency; that is, the error associated with the energy of an $\mathbb{N}$-particle system is *not* proportional to the number of particles in the limit $\mathbb{N} \to \infty$. In other words, for an ensemble of isolated molecules, the error in the truncated CI energy of the total ensemble is not the sum of the errors associated with the individual molecule energies [105]. Quadratic CI (QCI), a method containing quadratic terms in the configuration coefficients, does recover size consistency [105]. A related approach that also offers a size-consistent solution to the

electronic problem is the *coupled cluster* (CC) approximation [106]. In general, the equations required in CC theory are similar to those in QCI, but they are quartic in nature rather than quadratic, and thus, typically, computationally more demanding than the QCI equations.

Perturbation theory

An alternative approach that attempts to solve for the correlation energy in the electronic problem is Rayleigh-Schrödinger (RS) perturbation theory. This method is based on the division of the total Hamiltonian into two components, the zeroth-order part, $\hat{\mathbf{H}}_0$, and a small perturbation part, $\hat{\mathbf{H}}'$,

$$\hat{\mathbf{H}}_{el} = \hat{\mathbf{H}}_0 + \zeta\hat{\mathbf{H}}', \tag{2.53}$$

where $\zeta \ll 1$. The eigenvalue problem to be solved is then

$$\left(\hat{\mathbf{H}}_0 + \zeta\hat{\mathbf{H}}'\right)|\Phi_i\rangle = \mathcal{E}_i|\Phi_i\rangle. \tag{2.54}$$

Recalling the equation that needs to be solved, $\hat{\mathbf{H}}_{el}\Phi_{el} = \mathcal{E}_{el}\Phi_{el}$ (Eq. (2.4)), one can expand the exact electronic eigenfunctions, $|\Phi_i\rangle$, and eigenvalues, $\mathcal{E}_i$, in a Taylor series in the perturbation, ζ:

$$|\Phi_i\rangle = |\Psi_i\rangle + \zeta|\Psi_i^{(1)}\rangle + \zeta^2|\Psi_i^{(2)}\rangle + \cdots \tag{2.55}$$

$$\mathcal{E}_i = E_i^{(0)} + \zeta E_i^{(1)} + \zeta^2 E_i^{(2)} + \cdots . \tag{2.56}$$

It can be shown that for non-degenerate states, the nth order energy terms, $E_i^{(n)}$, can be expressed in terms of the appropriate perturbation matrix elements (where $|\Psi_i\rangle$ is written $|i\rangle$ for compactness) [99],

$$E_i^{(0)} = \langle i|\hat{\mathbf{H}}_0|i\rangle \tag{2.57}$$

$$E_i^{(1)} = \langle i|\hat{\mathbf{H}}'|i\rangle \tag{2.58}$$

$$E_i^{(2)} = \langle i|\hat{\mathbf{H}}'|i^{(1)}\rangle = \sum_{n\neq i}\frac{\langle i|\hat{\mathbf{H}}'|n\rangle\langle n|\hat{\mathbf{H}}'|i\rangle}{E_i^{(0)} - E_n^{(0)}} \tag{2.59}$$

$$\begin{aligned} E_i^{(3)} &= \langle i|\hat{\mathbf{H}}'|i^{(2)}\rangle \\ &= \sum_{m,n\neq i}\frac{\langle i|\hat{\mathbf{H}}'|n\rangle\langle n|\hat{\mathbf{H}}'|m\rangle\langle m|\hat{\mathbf{H}}'|i\rangle}{(E_i^{(0)} - E_n^{(0)})(E_i^{(0)} - E_m^{(0)})} \\ &\quad - E_i^{(1)}\sum_{n\neq i}\frac{\left|\langle i|\hat{\mathbf{H}}'|n\rangle\right|^2}{\left[E_i^{(3)} - E_n^{(0)}\right]^2} \end{aligned} \tag{2.60}$$

$$\vdots$$

where the exact forms of $|\Psi_i^{(n)}\rangle$ can be derived for a given $\hat{\mathbf{H}}'$ [99]. If the unperturbed Hamiltonian is just the sum of the N one-electron Fock operators, as suggested by Møller and Plesset (MP) [107],

$$\hat{\mathbf{H}}_0 \equiv \sum_{i=1}^{N} \hat{\mathbf{f}}(\vec{x}_i), \tag{2.61}$$

then the known eigenfunctions and eigenvalues, ε_i, are given by,

$$\hat{\mathbf{H}}_0 \Psi_0 = \left(\sum_{i=1}^{N} \varepsilon_i \right) \Psi_0 = E_0^{(0)} \Psi_0, \tag{2.62}$$

where ε_i are the orbital energies as defined in Eq. (2.29). The perturbation, $\zeta\hat{\mathbf{H}}'$, is the difference between the true molecular electronic Hamiltonian, $\hat{\mathbf{H}}_{el}$, and the unperturbed Hamiltonian. The first-order correction to the ground state energy, $E_0^{(1)}$, is given as

$$E_0^{(1)} = \langle \Psi_0^{(0)} | \hat{\mathbf{H}}' | \Psi_0^{(0)} \rangle \equiv \langle \Psi_0 | \hat{\mathbf{H}}' | \Psi_0 \rangle, \tag{2.63}$$

since $\Psi_0^{(0)}$=Ψ_0. Therefore,

$$\begin{aligned} E_0^{(0)} + E_0^{(1)} &= \langle \Psi_0^{(0)} | \hat{\mathbf{H}}_0 | \Psi_0^{(0)} \rangle + \langle \Psi_0^{(0)} | \hat{\mathbf{H}}' | \Psi_0^{(0)} \rangle \\ &= \langle \Psi_0 | \hat{\mathbf{H}}_0 + \hat{\mathbf{H}}' | \Psi_0 \rangle \\ &= \langle \Psi_0 | \hat{\mathbf{H}}_{el} | \Psi_0 \rangle. \end{aligned} \tag{2.64}$$

Notice that $\langle \Psi_0 | \hat{\mathbf{H}}_{el} | \Psi_0 \rangle$ is just the Hartree-Fock energy E_{HF} (see Eq. (2.45)), so

$$E_0^{(0)} + E_0^{(1)} = E_{HF}. \tag{2.65}$$

Therefore, the first *improvement* to the Hartree-Fock energy is the second-order energy, $E_0^{(2)}$, followed by higher-order terms. Recalling now the expression for the second-order energy, Eq. (2.59), the wave function $|i^{(1)}\rangle$ is just the determinant corresponding to the double excitation, $|\Psi_{ab}^{rs}\rangle$. Eq. (2.59) can therefore be rewritten,

$$E_0^{(2)} = \sum_{\substack{a<b \\ r<s}} \frac{|\langle ab||rs\rangle|^2}{\varepsilon_a + \varepsilon_b - \varepsilon_r - \varepsilon_s}, \tag{2.66}$$

where $a, b, \ldots$ and $r, s, \ldots$ correspond to occupied and virtual spin orbitals, respectively, The notation $\langle ab||rs\rangle$ represents the difference between two-electron integrals over spin orbitals,

$$\langle ab||rs\rangle = \langle ab|rs\rangle - \langle ab|sr\rangle \tag{2.67}$$

where $\langle ab|rs\rangle$ and $\langle ab|sr\rangle$ are defined in general as

$$\langle ij|kl\rangle = \int d\vec{x}_1 d\vec{x}_2 \chi_i^*(\vec{x}_1)\chi_j^*(\vec{x}_2) \frac{1}{\hat{\mathbf{r}}_{12}} \chi_k(\vec{x}_1)\chi_l(\vec{x}_2). \tag{2.68}$$

Computationally, MP energy calculations are performed in the following manner: a finite basis is chosen, and an SCF calculation is carried out to obtain Ψ_0, E_{HF}, and the virtual orbitals. If a complete set of basis functions would be taken, the SCF calculation would produce the exact Hartree-Fock energy and an infinite number of virtual orbitals. In reality, however, the basis set must be truncated, and a finite number of virtual orbitals are obtained, giving rise to the so-called "basis set truncation error". Next, $E^{(2)}$ and other higher order corrections are evaluated, where the sums, *e.g.* in Eq. (2.59), only run over a finite set of virtual orbitals. Typically, energy corrections beyond fourth-order are not considered due to the computational effort involved in calculating their contributions [103]. Another source of error arises when the *frozen-core* approximation is invoked to simplify the calculation of MP2, MP3, and MP4 energies; here, excitations of electrons from core orbitals are not considered. In addition, MPn perturbation theory is not variational and may yield an energy below the system's true energy. MP2, MP3, and MP4 methods are known to demonstrate oscillatory convergence behavior, and the calculated energies often overshoot the exact energy, as shown schematically in Figure 2.1 [103]. In fact, recent

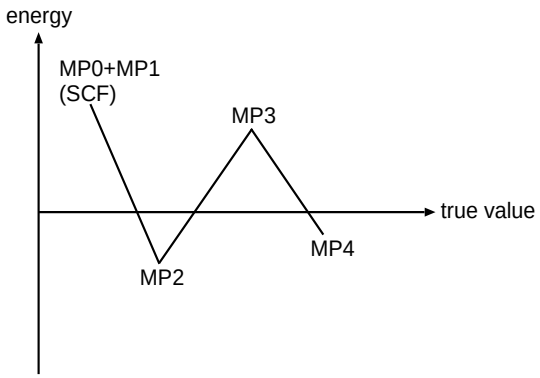

Figure 2.1: Oscillating convergence behavior of energy results obtained with the MPn method. The true energy is the exact non-relativistic electronic energy in the Born-Oppenheimer approximation.

studies of MP convergence behavior have shown that higher-order energy contributions can be quite unreliable and should only be included selectively [108]. Although not variational, an MPn series truncated at any order remains size-consistent. Size-consistency is generally considered to be more important than being variational, since one is often more interested in relative energy differences rather than in total energies [103]. Therefore, MPn is a popular method for calculating electronic energies, in particular MP2 or MP4.

2.2.2 Solving the nuclear problem

Having discussed some common methods for solving the electronic problem, we now return to the nuclear problem. Recall that the eigenvalues of the nuclear Hamiltonian are total

energies (Eq. (2.8)), composed of both electronic and nuclear contributions; the nuclear eigenfunctions $\Phi_{nuc}(\{\vec{R}_A\})$ are solved as functions of the nuclear coordinates $\{\vec{R}_A\}$ which also serve as parametric variables of the electronic function, $\Phi_{el}(\{\vec{r}_i\};\{\vec{R}_A\})$. Also, recall that the subsequent applications are for molecules or anions in the electronic ground state, so that the electronic quantum number $el=0$ has been dropped for simplicitiy of notation.

The nuclear problem itself can be divided into a two-part problem by considering the translational motion of the nuclei with respect to a space-fixed frame (*e.g.* the laboratory), and the internal motion (vibrations and rotations) with respect to the body-fixed frame of the nuclei [109]

$$\Phi_{nuc}(\{\vec{R}_A\}) = \Phi_{nuc}^{\text{trans}}(\{\vec{R}_{c.o.m.}\})\Phi_{nuc}^{\text{internal}}(\{\tilde{\vec{R}}_A\}), \tag{2.69}$$

with energies E^{trans} and E^{internal}, where $\vec{R}_{c.o.m.}$ denotes the (nuclear) center of mass, and $\tilde{\vec{R}}_A$ denotes the remaining "internal" nuclear degrees of freedom. The " ˜ " of $\tilde{\vec{R}}_A$ will be dropped subsequently for simplicity of notation. Typically, translational motion is described using the "particle-in-a-box" model, for which the potential energy within the box is zero and outside the box is infinite [109]. The translational energy of the molecule, E^{trans}, therefore only consists of kinetic energy that depends on the main quantum number n and inversely on size of the box,

$$E^{\text{trans}} = \frac{h^2}{8m}\left(\frac{\mathsf{n}_x^2}{\mathsf{a}^2} + \frac{\mathsf{n}_y^2}{\mathsf{b}^2} + \frac{\mathsf{n}_z^2}{\mathsf{c}^2}\right), \qquad \mathsf{n}_x, \mathsf{n}_y, \mathsf{n}_z = 1, 2, 3, \ldots \tag{2.70}$$

where a, b, and c are the lengths of the three-dimensional box and m is the mass of the system. The translational energy therefore adds a constant nonnegative energy to the total energy of the system [109].

Having treated the problem of translational motion separately, one can proceed to solve the Schrödinger equation for the internal motion of the nuclei, which consists of vibrational and rotational motion,

$$\hat{\mathbf{H}}_{nuc}^{\text{internal}}\Phi_{nuc}^{\text{internal}}(\{\vec{R}_A\}) = E^{\text{internal}}\Phi_{nuc}^{\text{internal}}(\{\vec{R}_A\}), \tag{2.71}$$

where

$$\hat{\mathbf{H}}_{nuc}^{\text{internal}} = \hat{\mathbf{T}}(\vec{R}_A) + \hat{\mathbf{V}}(\{\vec{R}_A\}), \tag{2.72}$$

where $\hat{\mathbf{T}}$ and $\hat{\mathbf{V}}$ are the operators of the kinetic and potential energies of the internal nuclear degrees of freedom, respectively. The energies in Eq. (2.71) are rotational-vibrational (ro-vibrational) eigenenergies. Typically, solving this problem (Eq. (2.71)) is non-trivial for molecules with more than two nuclei [110]. The centrifugal force arising from rotational motion causes internuclear distances to increase with increasing rotational frequency. Furthermore, the rotational constant of the molecule, B, depends

on the vibrational frequency ω, since the centrifugal force will be greater in the region near the equilibrium geometry [110].

A further simplification is thus often made, in which the function describing the internal motion, $\Phi_{nuc}^{\text{internal}}(\{\vec{R}_A\})$, is expressed as the product of vibrational and rotational wave functions [109],

$$\Phi_{nuc}^{\text{internal}}(\{\vec{R}_A\}) \approx \Phi_{nuc}^{\text{vib}}(\{\vec{R}_A\})\Phi_{nuc}^{\text{rot}}(\{\vec{R}_A\}), \tag{2.73}$$

with energies E^{vib} and E^{rot}. This separation of motion implies that Eq. (2.71) be split into two equations,

$$\hat{\mathbf{H}}_{nuc}^{\text{vib}}\Phi_{nuc}^{\text{vib}}(\{\vec{R}_A\}) = E^{\text{vib}}\Phi_{nuc}^{\text{vib}}(\{\vec{R}_A\}), \tag{2.74}$$

and

$$\hat{\mathbf{H}}_{nuc}^{\text{rot}}\Phi_{nuc}^{\text{rot}}(\{\vec{R}_A\}) = E^{\text{rot}}\Phi_{nuc}^{\text{rot}}(\{\vec{R}_A\}). \tag{2.75}$$

Since the rotational period is typically one hundred times longer than the vibrational period, ro-vibrational coupling is quite small and the separation of vibrational and rotational motion is a reasonable approximation [110]. In this approximation, the total internal energy is the sum of vibrational and rotational energy,

$$E^{\text{internal}} = E^{\text{vib}} + E^{\text{rot}}. \tag{2.76}$$

In the remainder of this thesis, vibrational and rotational motion will be treated separately. Rotational motion will be discussed in detail in Sections 2.5 and 2.5.3, focusing on the special case of a linear rigid molecule. In the next section, numerical methods for solving the vibrational problem will be discussed.

2.2.3 Numerical approaches to solving the vibrational problem

The Schrödinger equation describing the vibrations of nuclei can be solved exactly for simple models, such as the harmonic oscillator model. For real molecules, these models are insufficient at describing the potential energy of the system. Instead, numerical methods are needed to solve the nuclear Schrödinger equation. In this section we will therefore discuss one of the most common numerical approaches to solving the time-dependent nuclear Schrödinger equation, the Fourier grid Hamiltonian (FGH) [111, 112, 113].

The FGH method is a specific case of the discrete variable representation (DVR), a formalism that is based on choosing a convenient representation in which to diagonalize matrices of interest [114, 115]. For the sake of simplicity, a single particle of mass m moving in one linear dimension (r) will be considered, but the results may be extended

for systems with many degrees of freedom. The Hamiltonian for a particle of mass m can be written as

$$\begin{aligned} \hat{\mathbf{H}} &= \hat{\mathbf{T}} + \hat{\mathbf{V}}(r) \\ &= \frac{\hat{\mathbf{p}}^2}{2m} + \hat{\mathbf{V}}(r), \end{aligned} \tag{2.77}$$

where $\hat{\mathbf{p}} = -i\hbar\nabla$ is the momentum operator and $\hat{\mathbf{V}}(r)$ is the potential energy operator.

Discretization of space

Numerical methods for solving the nuclear Schrödinger equation typically rely on the discretization of position (r) and momentum space (k) into uniform segments, Δr or Δk, respectively [116]. Thus, a continuous range of r values is replaced by a grid of $\mathcal{N}$ discrete values, where the ith element is given as

$$r_i = i\Delta r \qquad \{i = 0, 1, \ldots, \mathcal{N}\}, \tag{2.78}$$

and where Δr is the uniform spacing between neighboring grid points and $\mathcal{N}$ is the total number of grid intervals. The total length of the grid is then given by $L = \mathcal{N}\Delta r$. The normalization condition holds for the wave function on the discretized grid as well,

$$\sum_{i=1}^{\mathcal{N}} \Psi^*(r_i)\Psi(r_i)\Delta r = \Delta r \sum_{i=1}^{\mathcal{N}} |\Psi(r_i)|^2 = 1. \tag{2.79}$$

The choice of grid size in coordinate space dictates the grid size in momentum space since the length L is inversely correlated with the wave number spacing Δk:

$$\Delta k = \frac{2\pi}{L}. \tag{2.80}$$

The central point is chosen as $k = 0$, and the grid points are distributed equally below and above zero. The minimum absolute value in momentum space is $k_{min} = (\mathcal{N}\pi/L)$, and the maximum absolute value is accordingly $k_{max} = (\mathcal{N}\pi/L)$. The momentum value at the jth discrete grid point is thus given by

$$k_j = j\Delta k - k_{min}. \tag{2.81}$$

Position and momentum space

We can now address the problem of representing the kinetic and potential energy operators, $\hat{\mathbf{T}}$ and $\hat{\mathbf{V}}$, in position and momentum space [112]. The kets of the coordinate space are the set $|r\rangle$ and they are eigenfunctions of $\hat{\mathbf{r}}$,

$$\hat{\mathbf{r}}|r\rangle = r|r\rangle \tag{2.82}$$

where the orthogonality and completeness relationships hold:

$$\langle r|r'\rangle = \delta(r - r') \tag{2.83}$$

and

$$\hat{\mathbf{1}}_r = \int_{-\infty}^{\infty} |r\rangle\langle r| dr. \tag{2.84}$$

The bras and kets of the discretized position space evaluate the wave function at the grid points,

$$\langle r_i|\Psi\rangle = \Psi(r_i) = (\Delta r)^{-1/2}\Psi_i, \tag{2.85}$$

where the orthogonality and completeness relationships (Eqs. (2.83) and (2.84)) can be rewritten,

$$\Delta r\langle r_i|r_q\rangle = \delta_{iq} \tag{2.86}$$

and

$$\hat{\mathbf{1}}_r = \sum_{i=1}^{\mathcal{N}} |r_i\rangle\Delta r\langle r_i|. \tag{2.87}$$

The potential energy is diagonal in the space spanned by $|r\rangle$,

$$\langle r'|\mathrm{V}(\hat{\mathbf{r}})|r\rangle = \mathrm{V}(r)\delta(r - r'). \tag{2.88}$$

The eigenfunctions of $\hat{\mathbf{p}}$ are the set of $|k\rangle$,

$$\hat{\mathbf{p}}|k\rangle = k\hbar|k\rangle \tag{2.89}$$

and they satisfy the orthogonality and completeness relationships,

$$\langle k|k'\rangle = \delta(k - k') \tag{2.90}$$

and

$$\hat{\mathbf{1}}_k = \int_{-\infty}^{\infty} |k\rangle\langle k| dk. \tag{2.91}$$

Therefore, the kinetic energy operator is diagonal in the momentum representation,

$$\begin{aligned} \langle k'|\hat{\mathbf{T}}|k\rangle &= T_k\delta(k - k') \\ &= \frac{\hbar^2 k^2}{2m}\delta(k - k'). \end{aligned} \tag{2.92}$$

The matrix elements responsible for transforming between the two representations are given as

$$\langle k|r\rangle = \frac{1}{(2\pi)^{1/2}} e^{(-ikr)}. \tag{2.93}$$

As a consequence, the wave function in position space is related to the wave function in momentum space via a Fourier transform:

$$\begin{aligned}\Psi(r) &= \langle r|\Psi\rangle \\ &= \langle r|\hat{\mathbf{1}}_k\Psi\rangle \\ &= \langle r|\left(\int_{-\infty}^{\infty}|k\rangle\langle k|dk\right)\Psi\rangle \\ &= \int_{-\infty}^{\infty}\langle r|k\rangle\langle k|\Psi\rangle\, dk\end{aligned}$$

$$\Psi(r) = \frac{1}{\sqrt{2\pi}}\int_{-\infty}^{\infty} e^{ikr}\Psi(k)\, dk. \tag{2.94}$$

Similarly, the wave function in momentum space can be expressed as the inverse Fourier transform of $\Psi(r)$:

$$\Psi(k) = \frac{1}{\sqrt{2\pi}}\int_{-\infty}^{\infty} e^{-ikr}\Psi(r)\, dr. \tag{2.95}$$

Remembering that $\hat{\mathbf{H}} = \hat{\mathbf{T}} + \hat{\mathbf{V}}(r)$,

$$\langle r|\hat{\mathbf{H}}|r'\rangle = \langle r'|\hat{\mathbf{T}}|r\rangle + \mathrm{V}(r)\delta(r-r')$$

and multiplying by $\hat{\mathbf{1}}_k$, one obtains

$$\langle r|\hat{\mathbf{H}}|r'\rangle = \int_{-\infty}^{\infty}\langle r|k\rangle\, T_k\, \langle k|r'\rangle dk + \mathrm{V}(r)\delta(r-r'). \tag{2.96}$$

Using Eq. (2.93), one can rearrange this result to obtain

$$\langle r|\hat{\mathbf{H}}|r'\rangle = \frac{1}{2\pi}\int_{-\infty}^{\infty} e^{ik(r-r')}\, T_k\, dk + \mathrm{V}(r)\delta(r-r'). \tag{2.97}$$

The kinetic energy operator is therefore applied in the following manner: first, the wave function is Fourier transformed (*cf.* Eq. (2.94)) from the position representation ($\Psi(r)$) to the momentum representation, ($\Psi(k)$). Second, the wave function is multiplied by $(\hbar\, k)^2/2m$ and inverse Fourier transform is carried out (*cf.* Eq. (2.95)). The potential energy is calculated by simply multiplying V with the value of $\Psi(r)$. The transformation between the two representations is most efficiently performed using fast Fourier transform (FFT) [117], an algorithm that is computationally more efficient than normal Fourier transform algorithm. Whereas basic FT computation time scales like $\mathcal{N}^2$ for $\mathcal{N}$ grid points, FFT scales like $\mathcal{N}\log_2\mathcal{N}$ [116]. Thus, the computational effort increases slowly

with the grid size. FFT benefits most from a system of $\mathcal{N} = 2^X$ points, where X is an integer [118]. The FGH method was used in our calculations, as implemented in the program *qmbound* [119], and the grids that are used accordingly consist of 2^X points.

Within the discretized grid of position or momentum space, the Hamiltonian elements of Eq. (2.97) can be rewritten:

$$\begin{aligned}
\langle r_i|\hat{\mathbf{H}}|r_j\rangle &= H_{ij} \\
&= \frac{1}{2\pi}\sum_{l=-n}^{n} e^{il\Delta k(r_i-r_j)}\left\{\frac{\hbar^2}{2m}(l\Delta k)^2\right\}\Delta k + \frac{\mathrm{V}(r_i)\delta_{ij}}{\Delta r} \\
&= \frac{1}{2\pi}\left(\frac{2\pi}{\mathcal{N}\Delta r}\right)\sum_{l=-n}^{n} e^{[il(2\pi/\mathcal{N}\Delta r)\times(i-j)\Delta r]}\cdot T_l + \frac{\mathrm{V}(r_i)\delta_{ij}}{\Delta r} \\
&= \frac{1}{\Delta r}\left\{\sum_{l=-n}^{n}\frac{e^{il2\pi(i-j)/\mathcal{N}}}{\mathcal{N}}\cdot T_l + \mathrm{V}(r_i)\delta_{ij}\right\}
\end{aligned} \tag{2.98}$$

where $n = (\mathcal{N}-1)/2$ and $\mathcal{N}$ now is an *odd* number of grid points in the spatial grid[1] and

$$T_l = \frac{\hbar^2}{2m}\cdot(l\Delta k)^2. \tag{2.99}$$

It should be noted that $T_0 = 0$. Combining the terms with negative and positive values of l, one arrives at

$$H_{ij} = \frac{1}{\Delta r}\left\{\frac{2}{\mathcal{N}}\sum_{l=1}^{n}\cos(l2\pi(i-j)/\mathcal{N})T_l + \mathrm{V}(r_i)\delta_{ij}\right\}. \tag{2.100}$$

The expectation values of the energies corresponding to $|\Psi\rangle$ are given as,

$$E = \frac{\langle\Psi|\hat{\mathbf{H}}|\Psi\rangle}{\langle\Psi|\Psi\rangle} = \frac{\sum_{ij}\Psi_i^*\Delta r H_{ij}\Delta r\Psi_j}{\Delta r\sum_i|\Psi_i|^2}. \tag{2.101}$$

Minimizing by applying the variational principle, one arrives at the secular equations,

$$\sum_j\left[H_{ij} - E_\upsilon\delta_{ij}\right]\Psi_j^\upsilon = 0, \tag{2.102}$$

which yield the bound-state vibrational eigenvalues, $(E^{\mathrm{vib}} =)E_\upsilon$, and the eigenvectors, Ψ_j^υ, which are the vibrational eigenfunctions as solutions of the vibrational Schrödinger equation (Eq. (2.74)) evaluated at the grid points.

[1] For an even number of grid points, see Ref. [111] for a more detailed discussion.

2.3 The time-dependent nuclear Schrödinger equation

In Section 2.2.2, the time-independent nuclear Schrödinger equation was introduced, and in Section 2.2.3, a numerical method (FGH) for obtaining the solutions to the vibrational problem was reviewed. The eigenfunctions of the time-independent vibrational Hamiltonian are *stationary* states. Here, stationary means the nuclei are fixed in space and that the energy of these states is constant. If, however, a quantum mechanical system interacts with an external force, such as electromagnetic radiation, the energy of the system will change with time. To obtain the time-dependent behavior of the system, the time-dependent nuclear Schrödinger equation (TDSE) must be solved. For this purpose, the time-dependent Hamiltonian and time-dependent Schrödinger equation will be presented in Section 2.3.1. In this context, we will also consider the TDSE for coupled molecular systems. Section 2.3.2 will examine the properties of an external electric field, and we will conclude with numerical methods for solving the TDSE in Section 2.3.5.

2.3.1 Time-dependent Hamiltonian

The time-dependent nuclear Schrödinger equation describes the evolution of a wave function in time:

$$i\hbar\frac{\partial}{\partial t}|\Psi_{tot}(t)\rangle = \hat{\mathbf{H}}(t)|\Psi_{tot}(t)\rangle, \tag{2.103}$$

The wave function $|\Psi_{tot}(t)\rangle$ is the total wave function for the system, which consists of a sum over all (orthonormal) electronic and nuclear wave functions,

$$\Psi_{tot}\left(\{\vec{r}_i\};\{\vec{R}_A\};t\right) = \sum_{el}\Phi_{el}\left(\{\vec{r}_i\};\{\vec{R}_A\}\right)\Phi^{el}_{nuc}\left(\{\vec{R}_A\};t\right). \tag{2.104}$$

From this point on, only the variable t will be retained in the notation, and the coordinates $\{\vec{r}_i\}$ and $\{\vec{R}_A\}$ will be dropped for simplicity of notation. One should remember that the electronic wave function depends on both electronic and nuclear coordinates $\left(\{\vec{r}_i\};\{\vec{R}_A\}\right)$ whereas the nuclear wave function depends on nuclear coordinates, as well as time $\left(\{\vec{R}_A\};t\right)$. The time-dependent Hamiltonian consists of the total molecular Hamiltonian, $\hat{\mathbf{H}}$, and a time-dependent potential energy term $\hat{\mathbf{V}}^{ext}(t)$ arising from the interaction of the molecular dipole moment $\vec{\boldsymbol{\mu}}$ with an external electromagnetic field $\vec{E}(t)$:

$$\hat{\mathbf{H}}(t) = \hat{\mathbf{H}} - \underbrace{\vec{\boldsymbol{\mu}}\cdot\vec{E}(t)}_{\hat{\mathbf{V}}^{ext}}. \tag{2.105}$$

Recall that the total Hamiltonian, $\hat{\mathbf{H}}$, defined in Eq. (2.2), consists of kinetic and potential energy for all nuclei and electrons. The total dipole moment, $\vec{\boldsymbol{\mu}}$, consists of the electronic and nuclear dipole moments, and it is given by

$$\vec{\boldsymbol{\mu}} = \underbrace{\sum_{i=1}^{N}(-e)\vec{r}_i}_{\vec{\boldsymbol{\mu}}_{el}} + \underbrace{\sum_{A=1}^{M}(Z_A e)\vec{R}_A}_{\vec{\boldsymbol{\mu}}_{nuc}}, \tag{2.106}$$

where $\vec{r}_i$ are position vectors of the electrons, and $\vec{R}_A$ are position vectors of the nuclei, from an origin in the frame of the molecule to the ith electron or Ath nucleus, respectively [99]. The term $\sum_{i=1}^{N}(-e)\,(\vec{r}_i)$ is the electric dipole operator, and it is a sum of one-electron operators.

Substitution of Eq. (2.104) into Eq. (2.103) leads to

$$i\hbar \sum_{el} |\Phi_{el}\rangle \frac{\partial}{\partial t} |\Phi_{nuc}^{el}(t)\rangle = \sum_{el} \hat{\mathbf{H}}(t)|\Phi_{el}\rangle|\Phi_{nuc}^{el}(t)\rangle. \tag{2.107}$$

Operating with $\langle\Phi_{el'}|$ on Eq. (2.107) gives

$$\langle\Phi_{el'}|i\hbar \sum_{el} |\Phi_{el}\rangle \frac{\partial}{\partial t} |\Phi_{nuc}^{el}(t)\rangle = \sum_{el} \langle\Phi_{el'}|\hat{\mathbf{H}}(t)|\Phi_{el}\rangle|\Phi_{nuc}^{el}(t)\rangle. \tag{2.108}$$

Due to the orthonormality of the electronic states, *i.e.* $\langle\Phi_{el'}|\Phi_{el}\rangle = \delta_{elel'}$, Eq. (2.108) reduces to

$$i\hbar \frac{\partial}{\partial t} |\Phi_{nuc}^{el'}(t)\rangle = \sum_{el} \langle\Phi_{el'}|\hat{\mathbf{H}}(t)|\Phi_{el}\rangle|\Phi_{nuc}^{el}(t)\rangle. \tag{2.109}$$

The time-dependent Hamiltonian from Eq. (2.105) can be expanded in the following manner:

$$\hat{\mathbf{H}}(t) = \hat{\mathbf{H}}_{el} + \sum_{A=1}^{M}\sum_{B>A}^{M} \frac{Z_A Z_B e^2}{4\pi\varepsilon_0 R_{AB}} + \hat{\mathbf{T}}_{nuc} - \vec{\boldsymbol{\mu}}_{el}\cdot\vec{E}(t) - \vec{\boldsymbol{\mu}}_{nuc}\cdot\vec{E}(t). \tag{2.110}$$

Therefore, the right-hand side of Eq. (2.109) consists of the following matrix elements:

$$\sum_{el}\langle\Phi_{el'}|\hat{\mathbf{H}}(t)|\Phi_{el}\rangle|\Phi_{nuc}^{el}(t)\rangle = \left[\hat{\mathbf{V}}_{el}\delta_{el'el} - \langle\Phi_{el'}|\vec{\boldsymbol{\mu}}_{el}|\Phi_{el}\rangle\cdot\vec{E}(t) - \vec{\boldsymbol{\mu}}_{nuc}\delta_{el'el}\cdot\vec{E}(t)\right]|\Phi_{nuc}^{el}(t)\rangle + \langle\Phi_{el'}|\hat{\mathbf{T}}_{nuc}|\Phi_{el}\rangle|\Phi_{nuc}^{el}(t)\rangle. \tag{2.111}$$

The electronic potential energy matrix elements are diagonal and vanish for $el \neq el'$, as do the nuclear dipole moment terms $\vec{\boldsymbol{\mu}}_{nuc}\delta_{el'el}$. Evaluation of the term $\langle\Phi_{el'}|\hat{\mathbf{T}}_{nuc}|\Phi_{el}\rangle|\Phi_{nuc}^{el}(t)\rangle$

gives rise to three sets of terms:

$$\begin{aligned}\langle\Phi_{el'}| - \frac{\hbar}{2}\sum_A \frac{{\nabla_A}^2}{m_A}|\Phi_{el}\rangle|\Phi^{el}_{nuc}(t)\rangle = &-\frac{\hbar^2}{2}\sum_A \frac{{\nabla_A}^2}{m_A}\delta_{elel'}|\Phi^{el}_{nuc}(t)\rangle \\ &- \hbar^2\sum_A \frac{1}{m_A}\underbrace{\langle\Phi_{el'}|\nabla_A|\Phi_{el}\rangle\nabla|\Phi^{el}_{nuc}(t)\rangle}_{\text{diabatic coupling}} \\ &- \frac{\hbar^2}{2}\sum_A \frac{1}{m_A}\underbrace{\langle\Phi_{el'}|{\nabla_A}^2|\Phi_{el}\rangle|\Phi^{el}_{nuc}(t)\rangle}_{\text{diabatic coupling}}.\end{aligned} \tag{2.112}$$

From the three nuclear kinetic terms on the right-hand side of Eq. (2.112), the second and third terms represent diabatic couplings of first and second order, respectively, between wave functions of different electronic states. These diabatic coupling terms are assumed to be small and will be neglected. We will therefore only retain the first nuclear kinetic term. Thus, the time-dependent Schrödinger equation can be written

$$\begin{aligned}i\hbar\frac{\partial}{\partial t}|\Phi^{el'}_{nuc}(t)\rangle &= \sum_{el}\langle\Phi_{el'}|\hat{\mathbf{H}}(t)|\Phi_{el}\rangle|\Phi^{el}_{nuc}(t)\rangle \\ &= \left[\hat{\mathbf{V}}_{el}\delta_{el'el} - \langle\Phi_{el'}|\vec{\boldsymbol{\mu}}_{el}|\Phi_{el}\rangle\cdot\vec{E}(t) - \vec{\boldsymbol{\mu}}_{nuc}\delta_{el'el}\cdot\vec{E}(t)\right]|\Phi^{el}_{nuc}(t)\rangle \\ &\quad -\frac{\hbar^2}{2}\sum_A \frac{{\nabla_A}^2}{m_A}\delta_{elel'}|\Phi^{el}_{nuc}(t)\rangle.\end{aligned} \tag{2.113}$$

One sees from Eq. (2.113) that the only coupling between different electronic states arises due to the electronic dipole moment $\vec{\boldsymbol{\mu}}_{el}$. Its off-diagonal matrix elements are accordingly referred to as the transition dipole moments.

Finally, Eq. (2.113) can be conveniently recast in matrix form for n electronic states:

$$i\hbar\frac{\partial}{\partial t}\begin{pmatrix}|\Phi^0_{nuc}(t)\rangle\\ \vdots \\ |\Phi^n_{nuc}(t)\rangle\end{pmatrix} = \begin{pmatrix}\hat{\mathbf{H}}_{00}(t) & \cdots & \hat{\mathbf{H}}_{0n}(t)\\ \vdots & \ddots & \vdots \\ \hat{\mathbf{H}}_{n0}(t) & \cdots & \hat{\mathbf{H}}_{nn}(t)\end{pmatrix}\begin{pmatrix}|\Phi^0_{nuc}(t)\rangle\\ \vdots \\ |\Phi^n_{nuc}(t)\rangle\end{pmatrix}. \tag{2.114}$$

Eq. (2.114) represents a system of coupled linear differential equations of first order in t. The coupling between these equations arises due to the perturbation, or off-diagonal matrix elements $\hat{\mathbf{H}}_{ij}(t)$.

For the specific case of a two-level system, as used in the forthcoming simulations, the time-dependent Schrödinger equation is given as

$$i\hbar\begin{pmatrix}|\Psi^1_{nuc}(t)\rangle\\ |\Psi^2_{nuc}(t)\rangle\end{pmatrix} = \begin{pmatrix}\hat{\mathbf{H}}_{11}(t) & \hat{\mathbf{H}}_{12}(t)\\ \hat{\mathbf{H}}_{21}(t) & \hat{\mathbf{H}}_{22}(t)\end{pmatrix}\begin{pmatrix}|\Psi^1_{nuc}(t)\rangle\\ |\Psi^2_{nuc}(t)\rangle\end{pmatrix}. \tag{2.115}$$

Now, the wave function $|\Phi^{el}_{nuc}(t)\rangle$ is replaced with $|\Psi^{el}_{nuc}(t)\rangle$ to emphasize that wave function is no longer the exact nuclear wave function. The Hamiltonian matrix is given as

$$\hat{\mathbf{H}}(t) = \begin{pmatrix} \hat{\mathbf{T}}_{11} + \hat{\mathbf{V}}_{11} - \vec{\boldsymbol{\mu}}_{11} \cdot \vec{E}(t) & -\vec{\boldsymbol{\mu}}_{12} \cdot \vec{E}(t) \\ -\vec{\boldsymbol{\mu}}_{21} \cdot \vec{E}(t) & \hat{\mathbf{T}}_{22} + \hat{\mathbf{V}}_{22} - \vec{\boldsymbol{\mu}}_{22} \cdot \vec{E}(t) \end{pmatrix}. \tag{2.116}$$

The diagonal dipole moment terms, $\vec{\boldsymbol{\mu}}_{ii}$, correspond to permanent dipole moments, whereas the off-diagonal dipole terms, $\vec{\boldsymbol{\mu}}_{ij}$, correspond to transition dipole moment terms between different electronic states. All of these matrix elements will be discussed in more detail in Section 4.2.

Time evolution operator, $\hat{\mathbf{U}}$

The TDSE can be solved using a unitary time evolution operator $\hat{\mathbf{U}}$ that propagates the wave function from time t_0 to t_1 [120]:

$$|\Psi(t_1)\rangle = \hat{\mathbf{U}}(t_1, t_0)|\Psi(t_0)\rangle, \tag{2.117}$$

where the $\hat{\mathbf{U}}$ has the property $\hat{\mathbf{U}}(t_0, t_0) = \hat{\mathbf{1}}$ and the group property that $\hat{\mathbf{U}}(t_0, t_2) = \hat{\mathbf{U}}(t_0, t_1)\hat{\mathbf{U}}(t_1, t_2)$. Eq. (2.117) can now be substituted in the TDSE (Eq. 2.103). Since any initial vector $|\Psi(t_0)\rangle$ must satisfy Eq. (2.103), the TDSE can also be recast with just the time evolution operator as the initial state [121]:

$$i\hbar\frac{\partial}{\partial t}\hat{\mathbf{U}}(t, t_0) = \hat{\mathbf{H}}(t)\hat{\mathbf{U}}(t, t_0). \tag{2.118}$$

Integration from t_0 to t leads to the following:

$$\begin{aligned} \hat{\mathbf{U}}(t, t_0) - \hat{\mathbf{U}}(t_0, t_0) &= -\frac{i}{\hbar}\int_{t_0}^{t} \hat{\mathbf{H}}(t_1)\hat{\mathbf{U}}(t_1, t_0)dt_1 \\ \hat{\mathbf{U}}(t, t_0) &= \hat{\mathbf{1}} - \frac{i}{\hbar}\int_{t_0}^{t} \hat{\mathbf{H}}(t_1)\hat{\mathbf{U}}(t_1, t_0)dt_1 \end{aligned} \tag{2.119}$$

Eq. (2.119) is solved in the following manner. First, for small time steps $\Delta t = t - t_0$, one can substitute $\hat{\mathbf{U}}(t, t_0) \approx \hat{\mathbf{U}}(t_0, t_0) = \hat{\mathbf{1}}$ under the integral; the approximate $\hat{\mathbf{U}}(t, t_0)$ obtained is then iteratively re-substituted until convergence is achieved. This iteration results in a time-ordered power series in terms of $\hat{\mathbf{H}}$, such that the time evolution operator responsible for propagation of a time interval $\Delta t = t - t_0$ is given as:

$$\hat{\mathbf{U}}(t, t_0) = \hat{\mathbf{1}} - \frac{i}{\hbar}\int_{t_0}^{t} \hat{\mathbf{H}}(t_1)dt_1 + \left(\frac{i}{\hbar}\right)^2 \int_{t_0}^{t} \hat{\mathbf{H}}(t_1)dt_1 \int_{t_0}^{t_1} \hat{\mathbf{H}}(t_2)dt_2 + \cdots \tag{2.120}$$

The time ordered series in Eq. (2.120) can be rewritten as a sum over all n expansion powers:

$$\hat{\mathbf{U}}(t, t_0) = \hat{\mathbf{1}} + \sum_{n=1}^{\infty}\left(-\frac{i}{\hbar}\right)^n \int_{t_0}^{t} dt_n \int_{t_0}^{t_n} dt_{n-1} \cdots \int_{t_0}^{t_2} dt_1 \hat{\mathbf{H}}(t_n)\hat{\mathbf{H}}(t_{n-1}) \cdots \hat{\mathbf{H}}(t_1). \tag{2.121}$$

If the Hamiltonian operator is not explicitly a function of time, the expression for the time evolution operator (Eq. (2.120)) simplifies to

$$\hat{\mathbf{U}}(t,t_0) = e^{-\frac{i}{\hbar}\hat{\mathbf{H}}(t-t_0)} \qquad \text{for} \qquad \hat{\mathbf{H}} \neq \hat{\mathbf{H}}(t). \tag{2.122}$$

When this time-evolution operator is applied to a stationary state (eigenfunction of the Hamiltonian), the system's energy remains constant, and only the phase of the wave function changes according to the exponential term in Eq. (2.122):

$$\begin{aligned} \hat{\mathbf{U}}(t,t_0)|\Psi(t_0)\rangle &= e^{-\frac{i}{\hbar}\hat{\mathbf{H}}(t-t_0)}|\Psi(t_0)\rangle \\ &= \sum_j e^{-\frac{i}{\hbar}E_j(t-t_0)}|\psi_j\rangle \underbrace{\langle\psi_j|\Psi(t_0)\rangle}_{c_j(t_0)}, \end{aligned} \tag{2.123}$$

where in Eq. (2.123), the wave function $|\Psi(t)\rangle$ is expanded in a basis of eigenfunctions of the Hamiltonian, $|\psi_j\rangle$,

$$|\Psi(t)\rangle = \sum_j |\psi_j\rangle\langle\psi_j|\Psi(t)\rangle. \tag{2.124}$$

The set of $c_j(t_0)$ are the initial expansion coefficients of the wave function, and E_j are the eigenvalues of the Hamiltonian [121],

$$\hat{\mathbf{H}}|\psi_j\rangle = E_j|\psi_j\rangle. \tag{2.125}$$

Time-discretization

When the Hamiltonian operator is time-dependent, the TDSE is solved according to the power series shown in Eq. (2.120). However, for computational purposes, an approximation can be made in which the time interval $[t_0, t]$ is discretized into $\mathcal{N}$ equal time segments, with $\mathcal{N}\Delta t = t - t_0$. If the time interval Δt is chosen sufficiently small, the time-dependent Hamiltonian operator $\hat{\mathbf{H}}(t)$ can be considered constant within the time interval, and Eq. (2.119) can be written as [121]:

$$\hat{\mathbf{U}}(t_n, t_{n-1}) \approx \hat{\mathbf{1}} - \frac{i}{\hbar}\hat{\mathbf{H}}(t_n)\Delta t. \tag{2.126}$$

The result of applying this time evolution operator to an initial wave function $|\Psi(t_0)\rangle$ is the successive propagation of the function over a time interval of Δt,

$$|\Psi(t)\rangle = \hat{\mathbf{U}}(t,t_n)\hat{\mathbf{U}}(t_n,t_{n-1})\ldots\hat{\mathbf{U}}(t_1,t_0)|\Psi(t_0)\rangle, \tag{2.127}$$

where each time evolution operator is given according to Eq. (2.122),

$$\hat{\mathbf{U}}(t_i,t_{i-1}) = e^{-\frac{i}{\hbar}\hat{\mathbf{H}}(t_i-t_{i-1})} = e^{-\frac{i}{\hbar}\hat{\mathbf{H}}(t_i)\Delta t} \tag{2.128}$$

with

$$t_i - t_{i-1} = \Delta t. \tag{2.129}$$

Having discussed the solution to the time-dependent Schrödinger equation, we will now address the nature of the time-dependent external potential, $\hat{\mathbf{V}}^{ext}(t)$, namely the interaction of matter with an electromagnetic field.

2.3.2 The origin of $\hat{\mathbf{V}}^{ext}(t)$: interaction of the electric dipole with an electromagnetic field

Electric dipole approximation

Classically, electromagnetic radiation is considered to be an oscillating wave of electric and magnetic fields. For typical field-matter interactions in atomic and molecular physics, the wavelength of the incident radiation, λ, is much larger than atomic dimensions [122], which are characterized in terms of the Bohr radius a_0, *i.e.*

$$\lambda \gg a_0. \tag{2.130}$$

The inequality (2.130) implies that spatial variations in the electromagnetic field are negligible on the scale of atomic dimensions, and that the radiation can be considered uniform when interacting with the charged nucleus and electrons of the atom, molecule, or ion. This approximation is termed the *electric-dipole approximation*. Implicit in the electric-dipole approximation is also the fact that the electric-dipole interaction term is much larger than other field-matter interactions, including electric-quadrupole and magnetic-dipole interactions [122]. The electric-quadrupole and magnetic-dipole contributions are two orders of magnitude smaller than that of the electric-dipole, so these interactions are often neglected [123].[2] Accordingly, in the following discussion, we will only consider the system's electric dipole interaction with the electric field.

Dipole moment operator

Classically, the electric dipole operator[3], $\vec{\boldsymbol{\mu}}$, is a sum of discrete charge vectors,

$$\vec{\boldsymbol{\mu}} = \sum_p Q_p \vec{r}_p, \tag{2.131}$$

[2]Nuclear magnetic resonance (NMR) relies on the interaction of the magnetic field with the magnetic dipole moments of the nuclei.

[3]The dipole moment operator is a quantum mechanical operator, but the notation $\hat{\boldsymbol{\mu}}$ will be replaced in this discussion with the notation $\vec{\boldsymbol{\mu}}$ to emphasize the vector quality of the dipole moment.

where $\vec{r}_p$ are position vectors and Q_p is the charge of the pth particle [99]. The quantum mechanical nuclear dipole operator, introduced in Eq. (2.106), includes a contribution of N electrons with a charge of $-e$, and the contribution of M nuclei, with charge $Z_A e$, $\vec{\boldsymbol{\mu}} = \sum_{i=1}^{N}(-e)\vec{r}_i + \sum_{A=1}^{M}(Z_A e)\vec{R}_A$ [99]. Acting on the wave function of the electronic ground state, $|\Psi_0\rangle$, the permanent dipole moment can be calculated according to:

$$\vec{\boldsymbol{\mu}}_{00} = \langle\Psi_0|\sum_{i=1}^{N}(-e)\vec{r}_i|\Psi_0\rangle + \sum_{A=1}^{M}(Z_A e)\vec{R}_A. \tag{2.132}$$

The notation of the permanent dipole moment will be written from now on as $\vec{\boldsymbol{\mu}}_0$, that is $\vec{\boldsymbol{\mu}}_{00} \equiv \vec{\boldsymbol{\mu}}_0$. One should note that, like the electronic wave function Φ_{el} (see Eq. (2.5)), the electronic contribution to the dipole moment is calculated from integrals that depend explicitly on electronic coordinates, $\{\vec{r}_i\}$, but parametrically on nuclear coordinates, $\{\vec{R}_A\}$ [99]. $\vec{\boldsymbol{\mu}}_0$ can be decomposed into its Cartesian components, for example the $\mu_{0,x}$ component is given as

$$\mu_{0,x} = \langle\Psi_0|\sum_{i=1}^{N}(-e)x_i|\Psi_0\rangle + \sum_{A=1}^{M}(Z_A e)X_A. \tag{2.133}$$

For molecules with a net charge not equal to zero (anions and cations), the permanent dipole moment of the molecule depends on the coordinate system. In other words, the dipole moment of a charged species is not invariant upon translations. Therefore, in the case of anions and cations, the coordinate system is typically defined relative to the molecule's center of mass [67].

Field-matter interaction

Earlier, in Eq. (2.105), we stated that the time-dependent potential $\hat{\mathbf{V}}^{ext}(t)$ has the form, $\hat{\mathbf{V}}^{ext}(t) = -\vec{\boldsymbol{\mu}} \cdot \vec{E}(t)$, where $\vec{\boldsymbol{\mu}}$ is the dipole moment operator and $\vec{E}(t)$ is a time-dependent electric field. Let us now assume that the electric field takes the following form,

$$\vec{E}(t) = \vec{\varepsilon} E_0 \sin(\omega t + \varphi) \cdot s(t) \tag{2.134}$$

where $\vec{\varepsilon}$ is a unit vector in the polarization direction, E_0 is the maximum value of $\vec{E}$, ω is a constant angular frequency, φ is a phase that we will set to 0 for simplicity, and $s(t)$ is an envelope function that will be discussed in more detail in the upcoming section (Section 2.3.3). Then, $\hat{\mathbf{V}}^{ext}(t)$ can be recast as

$$\hat{\mathbf{V}}^{ext}(t) = -\vec{\boldsymbol{\mu}} \cdot \vec{\varepsilon} E_0 \sin(\omega t) \cdot s(t). \tag{2.135}$$

Recalling now that we wish to solve the time-dependent Schrödinger equation for a time-dependent Hamiltonian, $\hat{\mathbf{V}}^{ext}(t)$ is substituted into Eq. (2.103). The evolution of the wave function $|\Psi(t)\rangle$ is then determined using the time evolution operator, $\hat{\mathbf{U}} = e^{-\frac{i}{\hbar}\hat{\mathbf{H}}\Delta t}$.

2.3.3 Properties of the electric field

The electric field in quantum dynamical simulations is typically designed to perform a specific task, for example initiating a ro-vibrational or electronic transition. Studying wave packet dynamics, or the dynamics of non-stationary states, is particularly useful to understand the time-dependent evolution of a quantum mechanical system. In such studies, radiation—either in the form of continuous wave (cw) or short pulses—can be applied to create the wave packet(s) [124]. In this section, various electric field properties will be discussed, focusing on the design of ultrashort laser pulses. In the case in which the field is not cw but rather "pulsed", the envelope function $s(t)$ from Eq. (2.134) can take one of several forms, such as a Gaussian function,

$$s(t) = e^{-(t-t_0)^2/\sigma^2} \tag{2.136}$$

or $\sin^2$ function [125],

$$s(t) = \sin^2\left(\frac{\pi(t-t_0)}{t_p}\right). \tag{2.137}$$

In Eq. (2.136), the pulse is centered at the time $t = t_0$ and the full (temporal) width of $s(t)$ at half the maximum height (FWHM) is given by $2\sigma\sqrt{\ln 2}$. In Eq. (2.137), t_p is the total pulse duration and t_0 is the initial time, so the pulse is centered at $t_0 + t_p/2$. The pulsed laser field then is described as

$$\vec{E}(t) = \begin{cases} \vec{\varepsilon} E_0 \sin(\omega t + \varphi) \cdot s(t) & t_0 \leq t \leq (t_0 + t_p) \\ 0 & \text{otherwise} \end{cases} \tag{2.138}$$

Intensity

The maximum intensity of the light, $I_{\max}$, is related to the field strength $\vec{E}(t)$ through

$$I_{\max} = \epsilon_0 \, c \max |\vec{E}(t)|^2 = \epsilon_0 \, c \, {E_0}^2 \tag{2.139}$$

where ϵ_0 is the dielectric constant and c is the speed of light [126]. To avoid undesired dissociation or ionization processes, maximum laser field intensities in quantum dynamical simulations are kept below the so-called Keldysh limit, typically $I_{\max} < 10^{13}$ W/cm^2 [127].

The duration t_p of a laser pulse and the spectral width $\Delta\omega$ are related through a Fourier transform. In general, the time and frequency components of light build what is called a Fourier pair [128]:

$$f(t) = \frac{1}{\sqrt{2\pi}} \int_{-\infty}^{+\infty} \mathcal{F}(\omega) e^{i\omega t} d\omega, \qquad \mathcal{F}(\omega) = \frac{1}{\sqrt{2\pi}} \int_{-\infty}^{+\infty} f(t) e^{-i\omega t} dt, \tag{2.140}$$

where $f(t)$ is the function describing the electric field in the time domain ($\equiv E(t)$), and $\mathcal{F}(\omega)$ is the function describing the electric field in the frequency domain. The duration Δt and spectral width $\Delta\omega$ are related by Heisenberg's uncertainty principle,

$$\Delta t \Delta\omega \geq \frac{1}{2}, \tag{2.141}$$

where the equality in Eq. (2.141) is only reached with time and spectral envelopes of Gaussian form. In such a case, the pulse is called *Fourier-transform limited* [128] and is the shortest pulse possible. In general, however, pulses need not be Fourier-transform limited.

To apply these relationships to the design of ultrashort IR and UV laser pulses [128]: a 50 femtosecond ($\Delta t = 50 \times 10^{-15}$ s) Gaussian-shaped pulse has a minimum spectral bandwidth of $\Delta\omega = 53$ cm^{-1}. If the central carrier frequency is in the IR range, *i.e.* $\omega = 1516$ cm^{-1} (corresponding to a laser wavelength $\lambda \sim 1064$ nm), the frequency bandwidth is $\Delta\omega/\omega \approx 0.03$. A pulse lasting 5 femtoseconds ($\Delta t = 5 \times 10^{-15}$ s) has a minimum spectral bandwidth of $\Delta\omega = 530$ cm^{-1}. If the central carrier frequency ω lies in the UV part of the electromagnetic spectrum, *i.e.* $\omega = 43\,500$ cm^{-1} (corresponding to a laser wavelength $\lambda \sim 230$ nm), then the frequency bandwidth is $\Delta\omega/\omega \approx 0.01$.

Few-cycle pulses

Few-cycle pulses are laser pulses whose envelope varies on a time scale comparable to that of the electromagnetic field itself [129]. The frequency of the radiation thus dictates the duration of the few-cycle pulse, depending on how many optical cycles are contained within the pulse envelope. Therefore, for a given number of cycles, the duration of a few-cycle IR pulse will necessarily be longer than that of a UV pulse. Current mode-locking techniques are able to deliver ∼4 fs pulses in the visible spectral region with only a single cycle [130]. For pulses on the order of 450 fs, high energy (0.8 μJ), half-cycle pulses can be generated [60].

A freely propagating electromagnetic pulse must integrate to zero, a condition that is a consequence of Maxwell's equations on electromagnetism in the electric dipole approximation [59, 131, 132],

$$\int_0^{t_p} E(t)dt = 0. \tag{2.142}$$

For pulses containing a large number of optical cycles within the pulse envelope, this condition is usually satisfied for any analytical expression describing the field since the average field strength is zero. For pulses containing a small number of optical cycles within the pulse envelope, any asymmetry in the electric field must be compensated by

pulse tails of opposite field strength. Few-cycle pulses that are created in the laboratory are accordingly preceded or followed by very long, weak intensity tails, whose amplitude is 10% or less of the amplitude of the main peaks [59]. These tails compensate for any peak area asymmetry and ensure that the total pulse area integrates to zero. Furthermore, the tails are spread over a long time period, such that they minimally affect the nature of the field-matter interaction that is determined by the central peaks. As a result, analytical expressions describing the laser field of few-cycle pulses often neglect these low-intensity tails, with the result that the total pulse area may not integrate to zero. In this thesis, we will use few-cycle pulses that are a good approximation to experimentally realistic pulses. Although the compensating long tails are neglected in the analytical pulse expressions, one can assume that their presence would not significantly change the nature of the field-matter interaction that has been modelled here.

2.3.4 Autocorrelation function and absorption cross-section

To monitor the evolution of the time-dependent wave function, one often considers the *autocorrelation function* $S(t)$ [133], a function that measures the overlap of the initial wave function with the time-dependent wave function $\Psi(t)$ at any time t:

$$S(t) \equiv \langle \Psi(t_0) | \Psi(t) \rangle. \tag{2.143}$$

If $\hat{\mathbf{H}}$ is time-independent, the wave packet $|\Psi(t)\rangle$ is obtained by operating on $|\Psi(t_0)\rangle$ with the time evolution operator, $\hat{\mathbf{U}} = e^{-i\hat{\mathbf{H}}(t-t_0)/\hbar}$ (for an extended discussion of $\hat{\mathbf{U}}$, see Section 2.3.1):

$$|\Psi(t)\rangle = e^{-i\hat{\mathbf{H}}(t-t_0)/\hbar} |\Psi(t_0)\rangle. \tag{2.144}$$

Substitution of Eq. (2.144) into Eq. (2.143) yields

$$S(t) = \langle \Psi(t_0) | e^{-i\hat{\mathbf{H}}(t-t_0)/\hbar} | \Psi(t_0) \rangle. \tag{2.145}$$

The modulus of the autocorrelation function, $|S(t)|$ is a real number whose value ranges from 0 to 1 for initially normalized wave functions. In general, the autocorrelation function is time-dependent. For example, consider a system at $t = 0$ that is a superposition of eigenfunctions $|\psi_j\rangle$ of the Hamiltonian, then $|\Psi(t_0)\rangle = \sum_j |\psi_j\rangle\langle\psi_j|\Psi(t_0)\rangle$ and

$$\begin{aligned} S(t) &= \langle \Psi(t_0) | e^{-i\hat{\mathbf{H}}(t-t_0)/\hbar} | \sum_j |\psi_j\rangle\langle\psi_j|\Psi(t_0)\rangle & (2.146) \\ &= \sum_j e^{-\frac{i}{\hbar}E_j(t-t_0)} \cdot |c_j(t_0)|^2. & (2.147) \end{aligned}$$

In the unique case in which the initial function $|\Psi(t_0)\rangle$ is itself an eigenstate of $\hat{\mathbf{H}}$ with energy E, then the autocorrelation function is just

$$S(t) = \langle \Psi(t_0) | \Psi(t_0) \rangle = e^{-iEt/\hbar} \tag{2.148}$$

and the modulus is unity for all times [134].

An application of the autocorrelation function is in the calculation of absorption and photodissociation cross sections. The absorption cross section $\sigma(\omega)$ is proportional to the Fourier transform of the dipole autocorrelation function [124]:

$$\sigma(\omega) \propto \int_{-\infty}^{+\infty} dt \, \underbrace{\langle \Psi(t) | \Psi(t_0) \rangle}_{S(t)} e^{i\omega t}, \tag{2.149}$$

where ω is the radiation frequency and the wave function of interest is the ket $|\Psi(t_0)\rangle$, defined as [135],

$$|\Psi(t_0)\rangle = \hat{\boldsymbol{\mu}} |\psi_0\rangle, \tag{2.150}$$

and $|\Psi(t)\rangle$ is given as

$$|\Psi(t)\rangle = e^{-\frac{i}{\hbar}\hat{\mathbf{H}}(t-t_0)} |\Psi(t_0)\rangle. \tag{2.151}$$

$|\psi_0\rangle$ is the zeroth nuclear wave function for the ground electronic potential energy surface, and $\hat{\boldsymbol{\mu}}$ is the vector dipole operator, either the permanent dipole operator $\hat{\boldsymbol{\mu}}_0$ in IR absorption processes, or the transition dipole operator $\hat{\boldsymbol{\mu}}_{fi}$ in UV absorption processes that couples an initial electronic state $|\Psi_i\rangle$ to a final electronic state $|\Psi_f\rangle$, *i.e.* $\hat{\boldsymbol{\mu}}_{fi} = \langle \Psi_f | \hat{\boldsymbol{\mu}} | \Psi_i \rangle$ [133]. For example, for the calculation of IR absorption spectra, the dipole autocorrelation function is,

$$S(t) = \langle \psi_0 | \hat{\boldsymbol{\mu}}_0 e^{-\frac{i}{\hbar}\hat{\mathbf{H}} t} \hat{\boldsymbol{\mu}}_0 | \psi_0 \rangle, \tag{2.152}$$

where $\hat{\mathbf{H}}$ is the full Hamiltonian for nuclear motion on the ground electronic state. Therefore, Eq. (2.149) relates the absorption cross section, with units of area, to the time evolution of the molecular system by a simple Fourier transform. By analyzing absorption and photodissociation cross sections, one can make quantitative predictions regarding line shapes and absorption envelopes of spectra [124].

2.3.5 Numerical methods for solving the time-dependent Schrödinger equation

We conclude this section with a discussion of numerical methods used to solve the time-dependent Schrödinger equation. Several numerical routines can be used to solve the time-dependent Schrödinger equation, including the method of finite differences, the Chebychev method [136], the Lanczos method [137], and the split-operator method [138, 139]. Here, we will only focus on the last method, the split-operator. We will conclude with a brief review of finite grids and the absorbing boundary method.

Split-operator method

The objective is the numerical propagation of $\Psi(t_0)$ to $\Psi(t_0+\Delta t)$, using the time evolution operator $\hat{\mathbf{U}}=e^{-\frac{i}{\hbar}\hat{\mathbf{H}}\Delta t}$:

$$\Psi(t_0+\Delta t)=e^{-\frac{i}{\hbar}\hat{\mathbf{H}}\Delta t}\Psi(t_0). \tag{2.153}$$

The main obstacle in solving this problem is that the kinetic energy operator is nonlocal in the position representation; in other words, although the potential energy $\hat{\mathbf{V}}$, which includes now the time-dependent operator $\hat{\mathbf{V}}^{ext}(t)$, is diagonal in position space, the kinetic energy operator $\hat{\mathbf{T}}$ is diagonal only in momentum space and the two quantities do not commute, $\left[\hat{\mathbf{T}},\hat{\mathbf{V}}\right]\neq 0$ [116, 117]. The term $e^{-\frac{i}{\hbar}\hat{\mathbf{H}}\Delta t}$ can therefore not be split into kinetic and potential terms:

$$e^{-\frac{i}{\hbar}\hat{\mathbf{H}}\Delta t}\neq e^{-\frac{i}{\hbar}\hat{\mathbf{T}}\Delta t}\cdot e^{-\frac{i}{\hbar}\hat{\mathbf{V}}\Delta t}. \tag{2.154}$$

Instead, an approximation is made that involves splitting the kinetic and potential energy operators in the following manner [116, 117]:

$$e^{\frac{-i}{\hbar}\Delta t\hat{\mathbf{H}}}=e^{\frac{-i}{2\hbar}\Delta t\hat{\mathbf{T}}}\cdot e^{\frac{-i}{\hbar}\Delta t\hat{\mathbf{V}}}\cdot e^{\frac{-i}{2\hbar}\Delta t\hat{\mathbf{T}}}+\mathcal{O}(\Delta t^3), \tag{2.155}$$

where the error $\mathcal{O}$ is third-order in the time increment, Δt. By choosing an adequately small time interval, one ensures that the time-dependent term $\hat{\mathbf{V}}^{ext}(t)$ arising from the electric field is constant, since it changes slowly during the time step. The propagation of the wave function for an interval Δt involves the following steps: beginning in position space, the wave function is Fourier-transformed to momentum space where it is multiplied by $\exp(-i\Delta t\hat{\mathbf{T}}/2\hbar)$; next, the function is transformed back to position space where it is multiplied by $\exp(-i\Delta t\hat{\mathbf{V}}/\hbar)$; finally, the function is transformed back to momentum space and multiplied again with $\exp(-i\Delta t\hat{\mathbf{T}}/2\hbar)$ before it is transformed back to coordinate space to complete one time step. Wave packet propagations discussed in this thesis were carried out using the split-operator method as described here [138, 139].

Since the split-operator method was introduced [138, 139], it has been improved by reducing the error to fourth-order in Δt [140]. The revised exponential split operator, containing seven exponential operators, is obtained by symmetrically splitting the exponential terms from Eq. (2.155) and is given as

$$e^{\eta(\hat{\mathbf{T}}+\hat{\mathbf{V}})}=e^{\frac{A\eta\hat{\mathbf{T}}}{2}}e^{A\eta\hat{\mathbf{V}}}e^{\frac{(1-A)\eta\hat{\mathbf{T}}}{2}}e^{(1-2A)\eta\hat{\mathbf{V}}}e^{\frac{(1-A)\eta\hat{\mathbf{T}}}{2}}e^{A\eta\hat{\mathbf{V}}}e^{\frac{A\eta\hat{\mathbf{T}}}{2}}+\mathcal{O}(\Delta t^4) \tag{2.156}$$

where $\eta=-i\Delta t/\hbar$ and $A=(2-2^{1/3})^{-1}$ [116, 140]. As a consequence of the third-order accuracy in Δt, larger time steps can be chosen for computational efficiency without sacrificing numerical stability.

Finite grid and absorbing boundary function

The time-dependent Schrödinger equation is solved numerically on a discretized grid of finite size. The grid length L in one dimension is given as $L = \mathcal{N}\Delta r$, where $\mathcal{N}$ is the number of grid intervals and Δr is the spacing between grid points, as discussed earlier in Section 2.2.3. This approach can be extended to a grid of multiple dimensions. The grid size is chosen to allow adequate representations of the time-dependent wave function in both position (r) and momentum (k) space. Under certain conditions, however, the wave packet may reach the boundary of the grid, either in position or momentum space. In momentum space, the maximum momentum can be extended by using a denser grid in position space, since $k_{max} \propto \mathcal{N}/L = 1/\Delta r$ [141]. Similarly, the range in position space can be extended by adding more grid points, but for a constant density of grid points, this extension could lead to a large and therefore computationally expensive number of grid points. One common method of circumventing this problem is to use an absorbing function at the boundary of the grid, also referred to as a "gobbler" function, $G(r_i)$, since it consumes outgoing wave packet fluxes. When chosen with the correct parameters, the gobbler function is a smooth absorbing function that prevents artificial reflection of the wave packet at the grid boundary [141, 116]. In this thesis, a Gaussian-shaped damping function was used to absorb outgoing wave packet fluxes in the wave packet propagations for the system OHF^-, as implemented in the program *qmpropa* [141]. In one dimension, the value of the gobbler function at the grid position r_i is given as

$$G(r_i) = \begin{cases} e^{-g_0(i-\mathcal{N}+g)^2} & i > \mathcal{N} - g \\ 1 & \text{otherwise,} \end{cases} \tag{2.157}$$

where g_0 is the damping constant, defined in this case as $g_0 = -\ln 10^{-4}/g^2$, and g is the parameter controlling the onset, and thus the smoothness, of the function. $\mathcal{N}$ is the number of grid points. The value of the wave function at the grid position r_i is then the product of the wave function and absorbing function,

$$\Psi(r_i) = \Psi(r_i) \cdot G(r_i). \tag{2.158}$$

On a 2D discretized grid, *i.e.* consisting of the grid points $\{r_i, r_j\}$, the Gaussian gobbler function is given as

$$G(r_i, r_j) = \begin{cases} e^{-g_0(i-\mathcal{N}_i+g)^2} \cdot e^{-g_0(j-\mathcal{N}_j+g)^2} & i > \mathcal{N}_i - g, j > \mathcal{N}_j - g \\ e^{-g_0(i-\mathcal{N}_i+g)^2} \cdot 1 & i > \mathcal{N}_i - g,\ j < \mathcal{N}_j - g \\ 1 \cdot e^{-g_0(j-\mathcal{N}_j+g)^2} & i < \mathcal{N}_i - g,\ j > \mathcal{N}_j - g \\ 1 & \text{otherwise.} \end{cases} \tag{2.159}$$

The value of the 2D wave function at the grid position $\{r_i, r_j\}$ is then given as

$$\Psi(r_i, r_j) = \Psi(r_i, r_j) \cdot G(r_i, r_j). \tag{2.160}$$

One sees from Eq. (2.159) that for small values of g, the damping function is largest for large values of r_i and r_j, and that it is zero for small values of r_i and r_j. Therefore, in asymptotic regions of the discretized potential energy surface, the damping function is largest to absorb outgoing wave packet fluxes.

2.4 Angular momentum

In Eq. (2.73), an approximation was made in which nuclear vibrational and rotational motions were separated; the internal nuclear wave function $\Phi_{nuc}^{\text{internal}}$ was expressed as a product of vibrational and rotational wave functions, $\Phi_{nuc}^{\text{internal}} \approx \Phi_{nuc}^{\text{vib}}\Phi_{nuc}^{\text{rot}}$. Having discussed numerical approaches to solving the vibrational problem in Section 2.2.3, our goal now is to examine the rotational nuclear wave function Φ_{nuc}^{rot} in more detail, specifically for the case of a rigid rotor. For this discussion, we will require a review of angular momentum. Therefore, in this section, we will begin with a review of the general theory of angular momentum in quantum mechanics (Section 2.4.1). Next, angular momentum algebra will be reviewed in the context of coupling two quantum mechanical angular momenta (Section 2.4.3). This review will highlight the Clebsch-Gordan coefficients and 3–J symbols, using the nomenclature of Zare [142].

2.4.1 Commutation rules

Let us define a generalized total angular momentum operator $\hat{\mathbf{J}}$ with three Cartesian components, $\hat{\mathbf{J}}_X$, $\hat{\mathbf{J}}_Y$, $\hat{\mathbf{J}}_Z$, which satisfy [142]:

$$\left[\hat{\mathbf{J}}_X, \hat{\mathbf{J}}_Y\right] = i\hbar\hat{\mathbf{J}}_Z \tag{2.161}$$

$$\left[\hat{\mathbf{J}}_Y, \hat{\mathbf{J}}_Z\right] = i\hbar\hat{\mathbf{J}}_X \tag{2.162}$$

$$\left[\hat{\mathbf{J}}_Z, \hat{\mathbf{J}}_X\right] = i\hbar\hat{\mathbf{J}}_Y, \tag{2.163}$$

i.e. the three components of $\hat{\mathbf{J}}$ do not commute with one another. The square of the total angular momentum operator $\hat{\mathbf{J}}$ can be defined as:

$$\hat{\mathbf{J}}^2 = \hat{\mathbf{J}}_X^2 + \hat{\mathbf{J}}_Y^2 + \hat{\mathbf{J}}_Z^2. \tag{2.164}$$

$\hat{\mathbf{J}}^2$ has the commutation properties:

$$\left[\hat{\mathbf{J}}^2, \hat{\mathbf{J}}_X\right] = 0 \tag{2.165}$$

$$\left[\hat{\mathbf{J}}^2, \hat{\mathbf{J}}_Y\right] = 0 \tag{2.166}$$

$$\left[\hat{\mathbf{J}}^2, \hat{\mathbf{J}}_Z\right] = 0, \tag{2.167}$$

which implies that it is possible to measure simultaneously $\hat{\mathbf{J}}^2$ and any *one* of the three components of $\hat{\mathbf{J}}$. Traditionally, $\hat{\mathbf{J}}_Z$ is specified along with $\hat{\mathbf{J}}^2$.

$\hat{\mathbf{J}}$ is Hermitian, so its eigenvalues are real; from Eq. (2.164), one can see that $\hat{\mathbf{J}}^2$ is just the sum of the squares of three Hermitian operators. This property implies that all the eigenvalues of $\hat{\mathbf{J}}^2$ are non-negative:

$$\begin{aligned}\langle\Psi|\hat{\mathbf{J}}^2|\Psi\rangle &= \langle\Psi|\hat{\mathbf{J}}_X^2|\Psi\rangle + \langle\Psi|\hat{\mathbf{J}}_Y^2|\Psi\rangle + \langle\Psi|\hat{\mathbf{J}}_Z^2|\Psi\rangle \\ &= ||\hat{\mathbf{J}}_X|\Psi\rangle||^2 + ||\hat{\mathbf{J}}_Y|\Psi\rangle||^2 + ||\hat{\mathbf{J}}_Z|\Psi\rangle||^2 \geq 0. \end{aligned} \tag{2.168}$$

Next, we will discuss the eigenvalues of the angular momentum operators.

2.4.2 Angular momentum observables

To begin, let us assume the total angular momentum $\hat{\mathbf{J}}$ is represented by a vector $\vec{\boldsymbol{J}}$ of indeterminate orientation on a cone of given side and height, shown in Figure 2.2. The

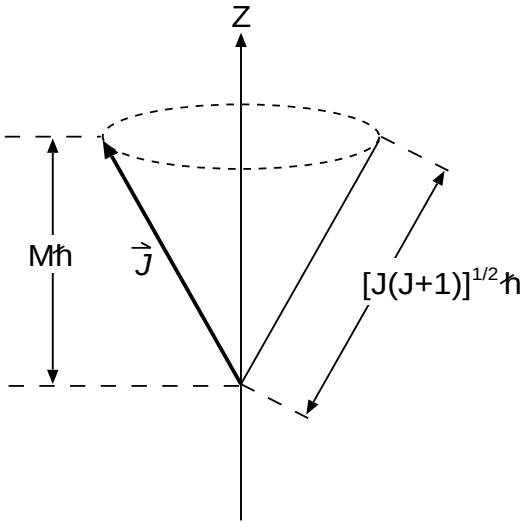

Figure 2.2: Vector representation of the total angular momentum $\vec{\boldsymbol{J}}$, whose magnitude is given by $[J(J+1)]^{1/2}\,\hbar$, and whose projection onto a space-fixed Z axis is given by $M\hbar$.

cone is positioned symmetrically about the space-fixed Z axis. The magnitude of the total angular momentum, $|\hat{\mathbf{J}}|$, is $[J(J+1)]^{1/2}\,\hbar$, as shown schematically in the vector representation[4] in Figure 2.2. The projection of the total angular momentum onto the space-fixed Z axis, is $M\hbar$, where M is a real, dimensionless number. This quantity is just the magnitude of the $\hat{\mathbf{J}}_Z$ component of the total angular momentum.

[4]One should distinguish the quantum mechanical angular momentum vector operator from a classical vector. The vector product of two classical vectors, $\vec{a}_1 \times \vec{a}_2 = a_1 a_2 \sin\theta$, where θ is the angle between the vectors $\vec{a}_1$ and $\vec{a}_2$, vanishes if $\vec{a}_2 = \vec{a}_1$. The product of two *vector operators*, however, is not zero, i.e. $\hat{\mathbf{J}} \times \hat{\mathbf{J}} = i\hbar\hat{\mathbf{J}}$ [143].

Whereas $M\hbar$ is the projection of the total angular momentum $\hat{\mathbf{J}}$ onto a space-fixed Z axis, a second projection can be considered, namely the projection of $\hat{\mathbf{J}}$ onto the z axis of a rigid body contained within the space-fixed frame, as shown in Figure 2.3. This

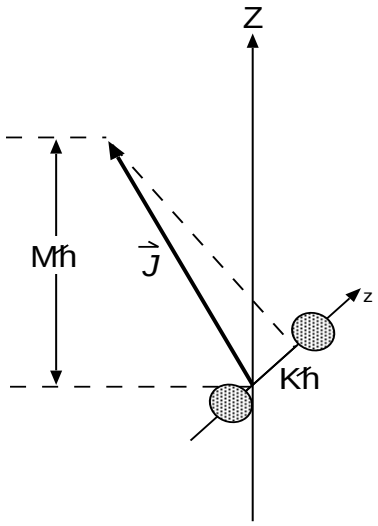

Figure 2.3: Vector representation of the total angular momentum vector $\vec{\boldsymbol{J}}$, and its projections $M\hbar$ and $K\hbar$ onto the space-fixed Z and body-fixed z axes, respectively.

projection of $\hat{\mathbf{J}}$ onto the *body-fixed* axis is $K\hbar$, where K, like M, is a real, dimensionless number. Together, the three quantum numbers J, K, and M constitute the $\{|J\,K\,M\rangle\}$ representation. Later, in Section 2.5.3, we will see how the set of $\{|J\,K\,M\rangle\}$ can be used to construct the wave functions of a rigid rotor. The eigenvalue equations of interest are:

$$\hat{\mathbf{J}}^2|J\,K\,M\rangle = J(J+1)\hbar^2|J\,K\,M\rangle \tag{2.169}$$

$$\hat{\mathbf{J}}_Z|J\,K\,M\rangle = M\hbar|J\,K\,M\rangle \tag{2.170}$$

$$\hat{\mathbf{J}}_z|J\,K\,M\rangle = K\hbar|J\,K\,M\rangle. \tag{2.171}$$

It can be shown that the possible values of J, M, and K are positive integers or half-integers, or zero [142]:

$$J = 0,\, 1/2\,,1,\, 3/2,\, 2\ldots \tag{2.172}$$

and that $(2J+1)$ possible values for M and K exist:

$$M = -J,\, -J+1,\, \ldots,\, J-1,\, J \tag{2.173}$$

$$K = -J,\, -J+1,\, \ldots,\, J-1,\, J. \tag{2.174}$$

Eigenvectors common to $\hat{\mathbf{J}}^2$, $\hat{\mathbf{J}}_Z$, and $\hat{\mathbf{J}}_z$ span the state space and satisfy the orthonormalization

$$\langle J\,K\,M|J'\,K'\,M'\rangle = \delta_{JJ'}\delta_{KK'}\delta_{MM'} \tag{2.175}$$

and closure relationships:

$$\sum_{J}\sum_{M=-J}^{J}\sum_{K=-J}^{J}|J\,K\,M\rangle\langle J\,K\,M| = 1. \tag{2.176}$$

At this point, having reviewed some fundamental relationships in the quantum mechanics of angular momentum, we turn our attention to the addition of angular momenta.

2.4.3 Coupling of two angular momentum vectors

In this section, we take advantage of the vector representation to illustrate the coupling of two quantum mechanical angular momenta. For clarity, we omit the vector notation and retain only the operator notation, $\hat{\mathbf{J}}$, to emphasize the quantum mechanical nature of these angular momenta. We are interested in the addition of two angular momentum vectors, as depicted schematically in Figure 2.4,

$$J = J_1 + J_2, \tag{2.177}$$

which also have M (projection onto a space-fixed Z axis) states associated with them, $|J_1M_1, J_2M_2\rangle$. (The following treatment is generalized for any vector and its components, so the coupling of two $|J\,K\rangle$ states is analagous and can be treated in the same manner.)

Coupled state

In Figure 2.4, J_1 and J_2 precess *in phase* (lower dashed circle) about J, while J precesses about the space-fixed Z axis (upper dashed circle). These components are said to be "coupled". At any time, the projection onto the space-fixed Z axis is M (up to a factor $\hbar$ which has been omitted in Figures 2.4 and 2.5 for clarity), but an indeterminacy exists in the values of M_1 and M_2. These coupled states, $J = J_1 + J_2$ and $M = M_1 + M_2$, are eigenfunctions of the momentum operators:

$$\hat{\mathbf{J}}^2|J_1J_2JM\rangle = J(J+1)\hbar^2|J_1J_2JM\rangle \tag{2.178}$$

$$\hat{\mathbf{J}}_Z|J_1J_2JM\rangle = M\hbar|J_1J_2JM\rangle \tag{2.179}$$

$$\hat{\mathbf{J}}_1^2|J_1J_2JM\rangle = J_1(J_1+1)\hbar^2|J_1J_2JM\rangle \tag{2.180}$$

$$\hat{\mathbf{J}}_2^2|J_1J_2JM\rangle = J_2(J_2+1)\hbar^2|J_1J_2JM\rangle \tag{2.181}$$

$$\tag{2.182}$$

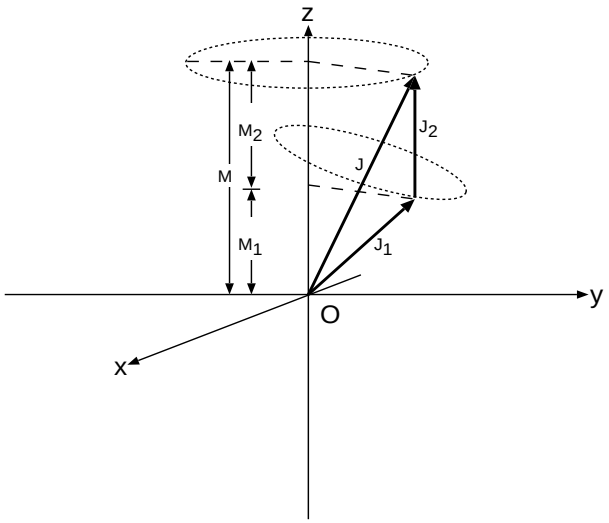

Figure 2.4: Vector representation of the *coupled* state $|JM\rangle$, where J is given as the vector sum of J_1 and J_2. The vectors J_1 and J_2 precess in phase about J (lower dashed circle), while the vector J precesses about the space-fixed Z axis (upper dashed circle). The projection (up to a factor $\hbar$) M is at any instant given as $M = M_1 + M_2$, although an indeterminancy in the individual components M_1 and M_2 exists (adapted from [142]).

Uncoupled state

In another representation, shown schematically in Figure 2.5, the vectors J_1 and J_2 precess independently about the space-fixed Z axis, each sweeping out a cone of its own. Accordingly, this representation is referred to as the "uncoupled" representation. At any instant, J_1 makes a projection M_1 and J_2 makes a projection M_2, but an indeterminacy in total M exists. These uncoupled states are eigenfunctions of the angular momentum operators,

$$\hat{\mathbf{J}}_1^2|J_1M_1, J_2M_2\rangle = J_1(J_1+1)\hbar^2|J_1M_1, J_2M_2\rangle \tag{2.183}$$

$$\hat{\mathbf{J}}_{1_Z}|J_1M_1, J_2M_2\rangle = M_1\hbar|J_1M_1, J_2M_2\rangle \tag{2.184}$$

$$\hat{\mathbf{J}}_2^2|J_1M_1, J_2M_2\rangle = J_2(J_2+1)\hbar^2|J_1M_1, J_2M_2\rangle \tag{2.185}$$

$$\hat{\mathbf{J}}_{2_Z}|J_1M_1, J_2M_2\rangle = M_2\hbar|J_1M_1, J_2M_2\rangle. \tag{2.186}$$

A unitary transformation connects the coupled and uncoupled representations,

$$|J_1J_2JM\rangle = \sum_{M_1,M_2} C(J_1J_2J; M_1M_2M)\,|J_1M_1, J_2M_2\rangle \tag{2.187}$$

where the coefficients—termed Clebsch-Gordan coefficients[5]—are defined as

$$C(J_1J_2J; M_1M_2M) \equiv \langle J_1M_1, J_2M_2|J_1J_2JM\rangle \equiv \langle J_1J_2JM|J_1M_1, J_2M_2\rangle. \tag{2.188}$$

[5]The Clebsch-Gordan coefficients are also sometimes referred to as vector coupling coefficients, vector addition coefficients, or Wigner coefficients.

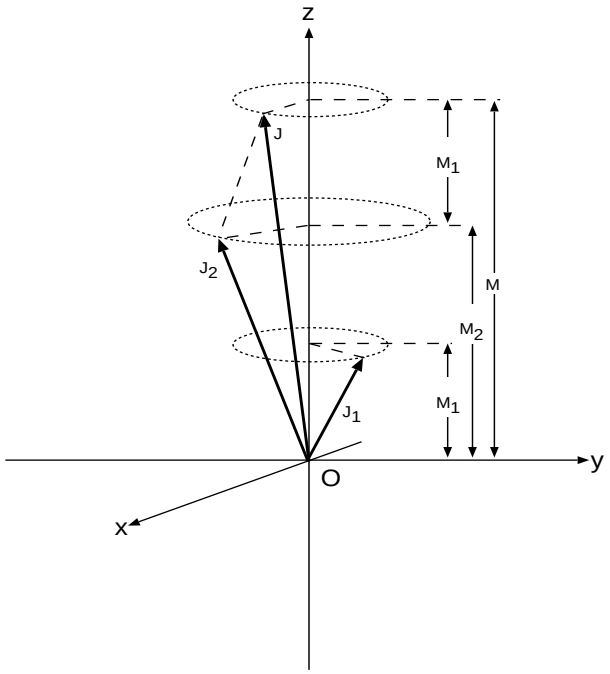

Figure 2.5: Vector representation of the *uncoupled* state $|JM\rangle$, where J_1 and J_2 precess independently about the space-fixed Z axis, making projections M_1 and M_2 (up to a factor $\hbar$). At any instant, the uncoupled state $|J_1\,M_1, J_2\,M_2\rangle$ couples to form the state $|J\,M\rangle$, with length $[J(J+1)]^{1/2}$ (adapted from [142]).

These coefficients form a unitary (orthogonal) matrix $\mathbf{C}$ of dimension $(2J_1+1)(2J_2+1)\times(2J_1+1)(2J_2+1)$. The orthonormality relationships hold:

$$\sum_{M_1,M_2}\langle J_1J_2JM|J_1M_1,J_2M_2\rangle\langle J_1M_1,J_2M_2|J_1'J_2'J'M'\rangle=\delta_{JJ'}\delta_{M,M'} \tag{2.189}$$

and

$$\sum_{J,M}\langle J_1M_1,J_2M_2|J_1J_2JM\rangle\langle J_1J_2JM|J_1M_1',J_2M_2'\rangle=\delta_{M_1,M_1'}\delta_{M_2,M_2'}. \tag{2.190}$$

Eqs. (2.189) and (2.190) demonstrate that the scalar product of any two column or row vectors vanishes, and the scalar product of any vector with itself is unity; $\mathbf{C}\mathbf{C}^{\mathbf{T}}=\hat{\mathbf{1}}$ and $\mathbf{C}^{\mathbf{T}}=\mathbf{C}^{-\mathbf{1}}$. In general, two conditions must be fulfilled for non-vanishing Clebsch-Gordan coefficients, namely

$$M=M_1+M_2 \tag{2.191}$$

and

$$|J_1+J_2|\geq J\geq|J_1-J_2|. \tag{2.192}$$

Eq. (2.192) is also referred to as the *triangle condition*. One should note that the magnetic quantum numbers M_1 and M_2 add algebraically whereas the angular momentum quantum

numbers J_1 and J_2 add vectorially (*cf.* Figure 2.4). An alternate representation of the Clebsch-Gordan coefficients are the Wigner 3–J symbols, defined as

$$\begin{pmatrix} J_1 & J_2 & J \\ M_1 & M_2 & M \end{pmatrix} \equiv (-1)^{J_1-J_2-M}(2J+1)^{-\frac{1}{2}}\langle J_1\, M_1, J_2\, M_2|J_1 J_2 J\ -M\rangle \tag{2.193}$$

or

$$\langle J_1\, M_1, J_2\, M_2|J_1 J_2 J\ -M\rangle \equiv (-1)^{J_1-J_2+M}(2J+1)^{\frac{1}{2}} \begin{pmatrix} J_1 & J_2 & J \\ M_1 & M_2 & M \end{pmatrix}. \tag{2.194}$$

The 3–J symbols are invariant under the cyclic exchange of any of the three columns. Under non-cyclic interchange of any two columns, or under sign reversal of M_1, M_2, and M_3, the 3–J symbol is multiplied by $(-1)^{J_1+J_2+J_3}$ [142]. Using the vector model for a geometric interpretation, one can consider the Clebsch-Gordan coefficients as indicating the possible angular momentum values that result after the addition of two angular momentum vectors, $J_1 + J_2$. The coefficient $\langle J_1 M_1, J_2 M_2|J_1 J_2 J\ -M\rangle$ represents the probability amplitude that the coupled state $|J_1 J_2 J\, M\rangle$ of length $[J(J+1)]^{1/2}$ will be found having its components J_1 and J_2 making the projection $M_1\hbar$ and $M_2\hbar$ for $\hat{\mathbf{J}}_{1_Z}$ and $\hat{\mathbf{J}}_{2_Z}$, respectively. The corresponding 3–J symbol is the probability amplitude divided by the factor $(2J+1)^{1/2}$. The squares of these coefficients represent probabilities, so they are real numbers whose values range from 0 to 1.

2.5 The rigid rotor

In this section, the rigid rotor will be presented as a model of the rotational dynamics of diatomic or linear polyatomic molecules. The standard rigid rotor eigenfunctions and eigenenergies will be reviewed in Section 2.5.1. In Section 2.5.2, the specific case of a linear triatomic molecule ABC will be treated. In this context, we will introduce (normalized) rotation matrices as rigid rotor wave functions. Finally, in Section 2.5.3, we will consider a rigid rotor in a linearly polarized laser field, focusing on the application to molecular orientation.

2.5.1 Wave functions and eigenenergies

A rigid (non-vibrating) diatomic molecule, or a linear polyatomic molecule, can be approximated as a rigid rotor. Due to the angular nature of the problem, spherical polar coordinates are optimal for describing the wave function, $\Psi(r, \theta, \phi)$. The transformation from Cartesian to spherical coordinates is sketched in Figure 2.6. The angle ϕ is the

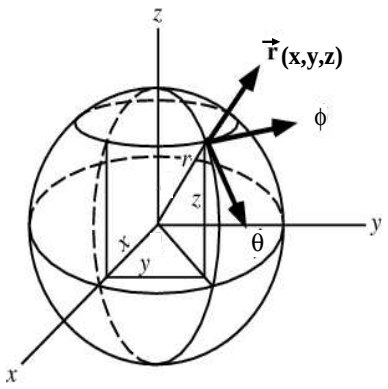

Figure 2.6: Sketch of spherical coordinates. The angle ϕ is the azimuthal angle in the x, y-plane from the x axis, with $0 \leq \phi \leq 2\pi$, θ is the polar angle from the z axis, with $0 \leq \theta \leq \pi$, and r is the distance from the point (x, y, z) to the origin.

azimuthal angle in the x, y-plane from the x axis with $0 \leq \phi \leq 2\pi$, θ is the polar angle from the z axis with $0 \leq \theta \leq \pi$, and r is the distance from the point (x, y, z) to the origin. Expressed in polar coordinates, the Cartesian coordinates (x, y, z) are

$$x = r \sin\theta \cos\phi, \qquad y = r \sin\theta \sin\phi, \qquad z = r \cos\theta. \tag{2.195}$$

In a rigid rotor, the internuclear bond distances are held constant, so its Hamiltonian only consists of kinetic energy due to the rotation of the molecule,

$$\hat{\mathbf{H}}_{r.r.} = -\frac{\hbar^2}{2\mu}\hat{\boldsymbol{\nabla}}^2, \tag{2.196}$$

where μ is the reduced mass of the two nuclei, and the Laplacian operator $\hat{\boldsymbol{\nabla}}^2$ is given by

$$\hat{\boldsymbol{\nabla}}^2 = \frac{1}{r}\frac{\partial^2}{\partial r^2}r + \frac{1}{r^2}\hat{\boldsymbol{\Lambda}}^2, \tag{2.197}$$

where $\hat{\boldsymbol{\Lambda}}^2$ is the Legendrian, or the angular portion of the Laplacian [143],

$$\hat{\boldsymbol{\Lambda}}^2 = \frac{1}{\sin^2\theta}\frac{\partial^2}{\partial\phi^2} + \frac{1}{\sin\theta}\frac{\partial}{\partial\theta}\sin\theta\frac{\partial}{\partial\theta}. \tag{2.198}$$

Since the radial coordinate r is constant in a rigid rotating molecule, the radial derivatives of $\hat{\boldsymbol{\nabla}}^2$ can be omitted,

$$\hat{\mathbf{H}}_{r.r.} = \frac{\hbar^2}{2\mu r^2}\underbrace{\left(-\frac{1}{\sin^2\theta}\frac{\partial^2}{\partial\phi^2} + \frac{1}{\sin\theta}\frac{\partial}{\partial\theta}\sin\theta\frac{\partial}{\partial\theta}\right)}_{\hat{\mathbf{J}}^2}. \tag{2.199}$$

The expression in parentheses in Eq. (2.199) is just the operator for the square of the total angular momentum in spherical polar coordinates, $\hat{\mathbf{J}}^2$, and the moment of inertia is $I = \mu r^2$, so the Hamiltonian for a rigid rotor can be written,

$$\hat{\mathbf{H}}_{r.r.} = \frac{\hbar^2}{2I}\hat{\mathbf{J}}^2. \tag{2.200}$$

The corresponding orthonormal eigenfunctions of the rigid rotor Hamiltonian are the spherical harmonics, $Y_J^M(\theta,\phi) \equiv |JM\rangle$, where J is the index corresponding to the total angular momentum, and M is the index of the magnetic quantum number. The spherical harmonics are defined only for integral values of J. In general, the total angular momentum J consists of the orbital angular momentum R due to the orbiting rigid body, the electronic orbital angular momentum, L, and the spin angular momentum, S:

$$J = R + L + S. \tag{2.201}$$

J is therefore a vector sum of all angular momenta, and it depends on the angles of rotation (θ,ϕ). The contribution of electronic orbital momentum (L) and spin angular momentum (S) to the total angular momentum J does not imply any vibronic coupling between nuclear and electronic modes. Furthermore, transitions between different electronic states are not considered here.

In the absence of spin, $S = 0$, for example for a singlet state, and in the absence

of electronic orbital momentum, $L = 0$, for example for a σ orbital, the total angular momentum quantum number, J, just consists of nuclear angular momentum, $J = R$. Initially, we limit the discussion of rigid rotor eigenfunctions and energy eigenvalues to the case of $S = 0$ and $L = 0$, but later we will return to this discussion and examine the rigid rotor wave functions for non-zero values of L. The spherical harmonics $Y_J^M(\theta, \phi)$ span an orthonormal set over the unit sphere,

$$\langle JM|J'M'\rangle = \int_0^{2\pi} d\phi \int_0^{\pi} d\theta \sin\theta Y_J^{M*}(\theta,\phi) Y_{J'}^{M'}(\theta,\phi) = \delta_{JJ'}\delta_{MM'}, \tag{2.202}$$

where $Y_J^{M*}(\theta, \phi) = (-1)^M Y_J^{-M}(\theta, \phi)$. The rotational energy levels E_J of a rigid rotor[6] are quantized according to,

$$E_J = \frac{\hbar^2}{2I} J(J+1). \tag{2.203}$$

It is customary to introduce a rotational constant, B, that is inversely proportional to I,

$$B = \frac{\hbar^2}{2I} \tag{2.204}$$

such that $E_J = BJ(J + 1)$. Thus, for a given J, E_J is $(2J + 1)$-fold degenerate. The separation of two adjacent rotational energy levels, $\Delta E_J = E_J - E_{J-1}$ is equal to:

$$\Delta E_J = B\left[J(J+1) - J(J-1)\right] = 2BJ \tag{2.205}$$

and increases linearly with J.

2.5.2 Linear triatomic molecule ABC

Next, we consider a specific rigid rotor, namely a triatomic linear molecule ABC with masses m_A, m_B, and m_C, and bonds of fixed length R_AB and R_BC, as shown in Figure 2.7. The rotation about the axis that passes the center of mass—which for asymmetric molecules is not the geometric center—will carry a moment of inertia I that is expressed in general as:

$$I = \sum_i m_i {R_i}^2 \tag{2.206}$$

where the mass m_i is located a radial distance R_i from the center of mass of the molecule. For a linear triatomic molecule ABC, it can be shown (see Appendix A for a complete derivation) that the moment of inertia is given as [144],

$$I_\mathrm{ABC} = m_\mathrm{A}{R_\mathrm{AB}}^2 + m_\mathrm{C}{R_\mathrm{BC}}^2 - \frac{1}{M}\left(m_\mathrm{A}R_\mathrm{AB} - m_\mathrm{C}R_\mathrm{BC}\right)^2. \tag{2.207}$$

where $M = m_\mathrm{A} + m_\mathrm{B} + m_\mathrm{C}$ and R_AB and R_BC are bond distances. Before discussing the

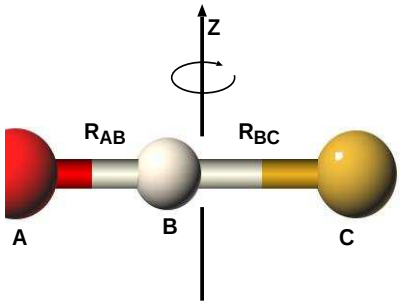

Figure 2.7: A rigid rotor model for a linear triatomic molecule consisting of masses m_{A}, m_{B}, and m_{C}, and bond lengths R_{AB} and R_{BC}. The rotation is about the axis that passes through the center of mass of the molecule, which for an asymmetric molecule, is not the geometric center.

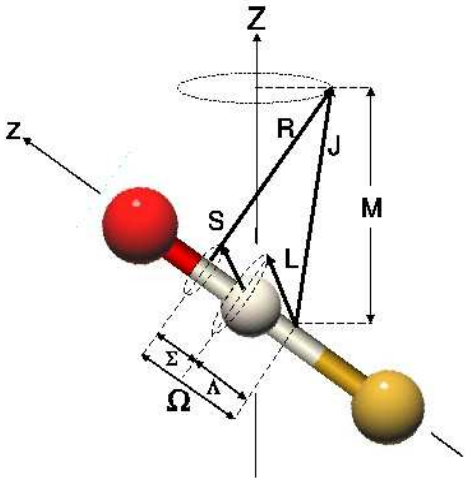

Figure 2.8: Vector representation of the components of rigid rotor angular momentum. $\hat{\mathbf{J}}$ is the total angular momentum, composed of orbital angular momentum due to the orbiting rigid body R, electronic angular momentum L, and spin angular momentum S. The projection of $\hat{\mathbf{J}}$ onto the space-fixed Z axis is M (up to a factor of $\hbar$), and the projection of $\hat{\mathbf{J}}$ onto the body-fixed z axis is Ω (up to a factor of $\hbar$), where Λ and Σ are the projections of L and S, respectively (adapted from [142]).

rigid rotor wave functions and energy eigenvalues, let us review the angular momentum components that contribute to J, by considering Figure 2.8. The total angular momentum, J, is composed of rotational angular momentum R arising from the orbiting rigid body, electronic orbital angular momentum, L, and spin angular momentum, S. The projection of J onto the space-fixed Z axis is quantized according to $M\hbar$, where M is the magnetic quantum number. Since the body-fixed z (molecular) axis is always perpendicular to the

[6]The commonly listed rigid rotor energy levels are only valid for the $^1\Sigma$ electronic state. For states with higher spin angular momentum or higher electronic orbital angular momentum, such as a $^2\Pi$ state, corrections must be made to the $^1\Sigma$ rigid rotor energies [142].

rotational angular momentum R in the case of a linear rigid rotor, the projection of R onto this axis is zero. Rather, the orbital electronic angular momentum, L, and the spin momentum, S, make projections $\Lambda\hbar$ and $\Sigma\hbar$, respectively, onto the body-fixed axis. The values of L range from $L=0,1,2,\ldots$ for $S,P,D,\ldots$ orbitals, and $\Lambda=\pm L$; $\Sigma=\pm\frac{1}{2},\pm 1,\ldots$ for a doublet, triplet, etc. The sum of Λ and Σ is termed Ω,

$$\Omega = \Lambda + \Sigma. \tag{2.208}$$

Let us recall now the eigenvectors of $\hat{\mathbf{J}}^2$, $\hat{\mathbf{J}}_Z$, and $\hat{\mathbf{J}}_z$, defined in Eqs. (2.169), (2.170), and (2.171), where J was the total angular momentum and $M\hbar$ and $K\hbar$ were projections thereof onto the space-fixed Z and body-fixed z axes, respectively. To reflect the fact that the system may have non-zero spin and non-zero electronic orbital angular momentum, the index K is often changed to Ω, *i.e.* $|J\,K\,M\rangle$ goes to $|J\,\Omega\,M\rangle$. With these tools in hand, we are now able to discuss the rigid rotor wave functions.

As discussed earlier, the spherical harmonics, $Y_J^M(\theta,\phi)$, are eigenfunctions of the rigid rotor Hamiltonian for integral values of J. An alternate, yet equivalent, formu-

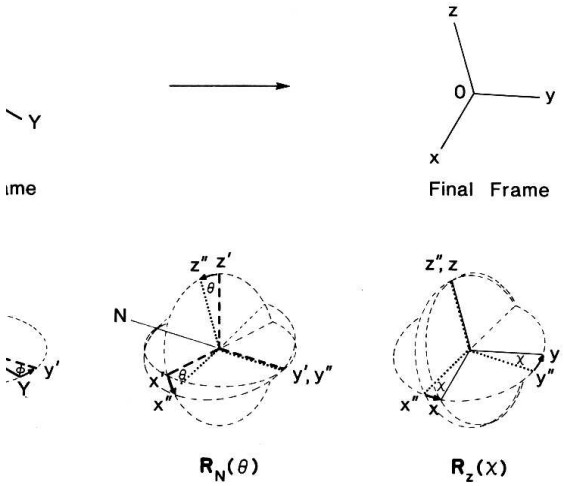

Figure 2.9: Rotation through the Euler angles (ϕ,θ,χ) transforms the space-fixed frame (X,Y,Z) into the molecule-fixed frame (x,y,z) (adapted from [142]). The transformation is accomplished with a rotation ϕ about the space-fixed Z axis, a rotation θ about the line of nodes N, and finally a rotation χ about the z axis.

lation for the rigid rotor wave functions is in terms of *rotation matrices*. A rotation matrix $\mathbf{R}(\phi,\theta,\chi)$ is a matrix that rotates one coordinate frame into another frame—in this case, the space-fixed (X,Y,Z) frame into the molecule-fixed (x,y,z) frame. This transformation, sketched in Figure 2.9, is accomplished by three successive finite rotations:

1. a counter-clockwise rotation ϕ about the space-fixed Z axis, which carries the Y axis into the line of nodes N

2. a counter-clockwise rotation θ about the line of nodes N, which carries the Z axis into the z axis

3. a counter-clockwise rotation χ about the z axis, which carries the line of nodes N into the y axis.

The Euler angles are therefore the angles through which a frame (X, Y, Z) must be turned in order to coincide with a frame (x, y, z), and the total transformation can be described as the product of three individual rotations:

$$\begin{aligned} \mathbf{R}(\phi, \theta, \chi) &= \mathbf{R}_z(\chi)\mathbf{R}_N(\theta)\mathbf{R}_Z(\phi) \\ &= e^{(-i\chi J_z)}e^{(-i\theta J_N)}e^{(-i\phi J_Z)} \end{aligned} \tag{2.209}$$

where for an arbitrary rotation about an axis $\vec{n}$ by an angle ξ, $\mathbf{R}_n(\xi)$ is given as

$$\mathbf{R}_n(\xi) = e^{-\frac{i}{\hbar}\xi \vec{J}\cdot\vec{n}} \tag{2.210}$$

and $\vec{J}\cdot\vec{n}$ is the component of $\vec{J}$ along the $\vec{n}$ axis. Here, the vector notation is used to emphasize the directionality of J. Eq. (2.209) is often recast in another form to avoid mixing operators belonging to different coordinate frames [142]. One convenient expression is

$$\mathbf{R}(\phi, \theta, \chi) = e^{(-i\phi J_Z)}e^{(-i\theta J_Y)}e^{(-i\chi J_Z)}, \tag{2.211}$$

which can be shown to perform a rotation identical to that performed in Eq. (2.209) [142].

Now, let us consider a rotation acting on the eigenstate $|J\,\Omega\,M\rangle$ of $\hat{\mathbf{J}}^2$ and $\hat{\mathbf{J}}_Z$, which transforms $|J\,\Omega\,M\rangle$ into a linear combination of other M values without changing J and Ω (the following discussion can be applied analogously to rotations that transform Ω to Ω'):

$$\mathbf{R}(\phi, \theta, \chi)|J\,\Omega\,M\rangle = \sum_{M'} D^J_{M'\,M}|J\,\Omega\,M'\rangle \tag{2.212}$$

where the expansion coefficients $D^J_{M'\,M}(\phi, \theta, \chi)$,

$$D^J_{M'\,M}(\phi, \theta, \chi) = \langle J\,\Omega\,M'|\mathbf{R}(\phi, \theta, \chi)|J\,\Omega\,M\rangle, \tag{2.213}$$

are the elements[7] of a $(2J + 1) \times (2J + 1)$ unitary rotation matrix, $\mathbf{R}$. Together, the rotation matrix acting on the wave function $|J\,\Omega\,M\rangle$, is still an eigenket of the operator

[7]The present derivation is adapted from Ref. [142]. We note that, paradoxically, the left-hand side of Eq. (2.213) does not depend on Ω, in contrast to the right-hand side.

$\hat{\mathbf{J}}^2$ with the same eigenvalues $J(J+1)\hbar^2$ [134]:

$$\hat{\mathbf{J}}^2\mathbf{R}(\phi,\theta,\chi)|J\,\Omega\,M\rangle = \mathbf{R}(\phi,\theta,\chi)\hat{\mathbf{J}}^2|J\,\Omega\,M\rangle \quad (2.214)$$

$$= J(J+1)\hbar^2\,\mathbf{R}(\phi,\theta,\chi)|J\,\Omega\,M\rangle. \quad (2.215)$$

The rotation matrix leaves the wave function unchanged, except possibly for a phase factor, such that the probability $|J\,\Omega\,M(\phi,\theta,\chi)|^2$ is conserved. The rotation coefficients $D^J_{M'\,M}(\phi,\theta,\chi)$ represent the probability amplitude that the projection $M\hbar$ of the angular momentum vector J in the original frame will be $M'\hbar$ after a rotation through the Euler angles (ϕ,θ,χ) [142]. Substitution of Eq. (2.209) into Eq. (2.213) gives

$$D^J_{M'\,M}(\phi,\theta,\chi) = e^{iM'\phi}d^J_{M'\,M}(\theta)e^{i\,M\chi}, \quad (2.216)$$

where

$$d^J_{M'\,M}(\theta) = \langle J\,\Omega\,M'|e^{-i\theta\,J_Y}|J\,\Omega\,M\rangle. \quad (2.217)$$

Eq. (2.216) was derived using the identity

$$e^{(-i\xi J_Z)}|J\,\Omega\,M\rangle = e^{(-i\xi M\hbar)}|J\,\Omega\,M\rangle. \quad (2.218)$$

The significance of the rotation $e^{-i\theta\,J_Y}$ is to mix different M values, so the evaluation of these matrix elements is nontrivial [134]. Typically, the expansion coefficients $d^J_{M'\,M}(\theta)$ are evaluated from a finite polynomial in arguments of the half angle $\theta/2$, and algebraic expressions for several common values of J and M have been tabulated (see *e.g.* Ref. [142]). For example, for $J=1$, $M=1$, and $M'=1$, $d^1_{11}(\theta)=\frac{1}{2}(1+\cos\,\theta)$. For $J=1$, $M=0$, and $M'=0$, $d^1_{00}(\theta)=\cos\,\theta$, which is just the spherical harmonic $Y^0_1(\theta,\phi)$, up to a factor of $\sqrt{(3/4\pi)}$ [142].

Particularly useful is the integral over a product of rotation matrices having the same angular arguments. These integrals can be conveniently evaluated with the help of $3-J$ symbols [142]:

$$\frac{1}{8\pi^2}\int_0^{2\pi}\int_0^{\pi}\int_0^{2\pi} D^{J_1}_{M_1'\,M_1}(\phi,\theta,\chi)D^{J_2}_{M_2'\,M_2}(\phi,\theta,\chi)D^{J_3}_{M_3'\,M_3}(\phi,\theta,\chi)d\phi\sin\theta d\theta d\chi$$
$$= \begin{pmatrix} J_1 & J_2 & J_3 \\ M_1' & M_2' & M_3' \end{pmatrix}\begin{pmatrix} J_1 & J_2 & J_3 \\ M_1 & M_2 & M_3 \end{pmatrix} \quad (2.219)$$

Finally, it can be shown that the general wave function for a rigid rotor is a linear combination of rotation matrices [142, 134]. In the case of a rigid rotor, only two rotational degrees of freedom exist and the third Euler angle χ can be fixed arbitrarily. By convention, χ is set to zero, such that (ϕ,θ,χ) can be written as $(\phi,\theta,0)$ [142]. Including a normalization factor, the rigid rotor wave functions $|J\,\Omega\,M\rangle$ are given as

$$|J\,\Omega\,M\rangle = \left[\frac{2J+1}{4\pi}\right]^{\frac{1}{2}} D^{J^*}_{\Omega\,M}(\phi,\theta,0) = \left[\frac{2J+1}{4\pi}\right]^{\frac{1}{2}}(-1)^{M-\Omega}D^J_{-\Omega\,-M}(\phi,\theta,0). \quad (2.220)$$

The expansion coefficients $D^J_{\Omega M}$ are now the coefficients of a rotation matrix that rotate the body-fixed frame (x, y, z) into coincidence with the space-fixed frame (X, Y, Z).

2.5.3 Orienting a linear rigid rotor in a laser field

Orientation versus alignment

Controlling the orientation of molecules in the laboratory frame is highly desirable for the optimization of bi-molecular collision experiments since the position of collision partners determines the outcome of the encounter. Likewise, in unimolecular dissociation experiments, controlling the orientation of molecules is essential for the spatial separation of dissociation products. Before continuing, it is instructive to distinguish between *alignment* and *orientation*. Alignment refers to the spatial distribution of *single-headed* arrows, whereas orientation refers to the preferential distribution of *double-headed* arrows [142]. In terms of momentum eigenfunctions, alignment is concerned with the population of $|J\,\Omega\,M\rangle$ and $|J\,\Omega\,{-M}\rangle$ versus $|J\,\Omega\,M'\rangle$ and $|J\,\Omega\,{-M'}\rangle$. Orientation, however, distinguishes between $|J\,\Omega\,M\rangle$ and $|J\,\Omega\,{-M}\rangle$, a population difference that gives rise to a net helicity or spin [142]. A polar linear molecule ABC, for example, can be considered a double-headed arrow, so its angular momentum distribution is best characterized in terms of orientation. A nonpolar molecule ABA could only be described in terms of alignment.

Half-cycle pulse (HCP)

In this section, we will consider a rigid rotor in the presence of a nonresonant, moderately intense ($I_{\max} \approx 10^8 - 10^{12}$ W/cm^2), linearly polarized half-cycle pulse (HCP). A HCP can be generated, such that it consists of a large (on the order of 5 : 1) asymmetry in the positive and negative electric field magnitudes [60]. The central peak is predominantly unipolar, and, in the laboratory, it is preceded or followed by long, low-intensity tails of opposite field strength, such that the total area under pulse integrates to zero [59]. These tails are on the order of ten times the length of the central peak. Such an experimentally reproducible pulse is shown in Figure 2.10 (solid line, adapted from Ref. [60]). The tail area, integrated up to $t = 4$ ps, represents 15% of the main peak area. Superimposed on the HCP in Figure 2.10 is a sine-square function (dashed line, taken from Ref. [59]). The sine-square pulse is a good approximation to the experimental HCP, despite the missing long weak tail. The inset (adapted from Ref. [60]) shows the Fourier transform of the HCP in the frequency (cm^{-1}) domain. In our simulations, we will also approximate a HCP without including the long tails of opposite field strength. Since the central peak is responsible for the significant transfer of angular momentum to the system, neglecting these low-intensity tails should be a valid approximation [59, 145]. For a general discussion on the design of few-cycle pulses, see Section 2.3.3.

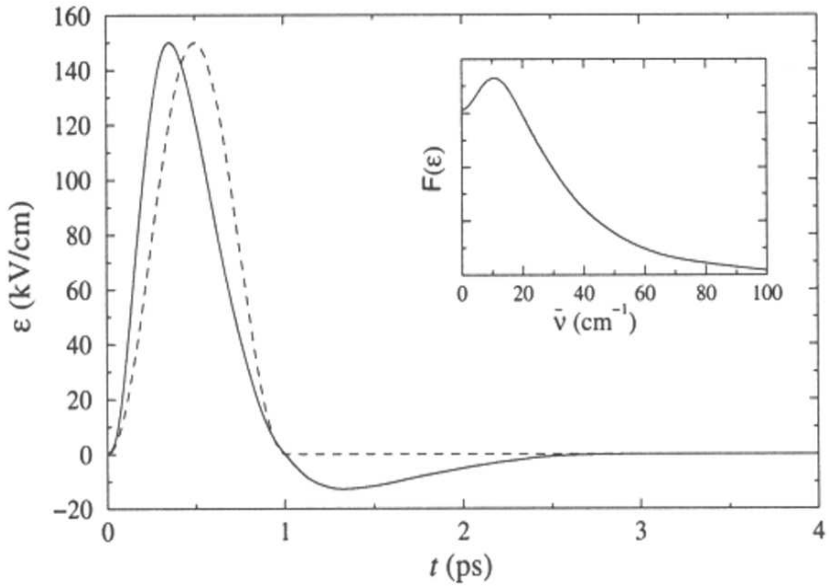

Figure 2.10: An experimentally reproducible HCP (solid line) and a sine-square function (dashed line) that is a good approximation of the HCP, adapted from Refs. [59] and [60]. The tail area of the experimental pulse, integrated up to $t = 4$ ps, represents 15% of the main peak area. The inset (adapted from Ref. [60]) shows the Fourier transform of the HCP in the frequency (cm^{-1}) domain.

Interacting with matter, the HCP exerts a unidirectional force on the molecular axis, similar to a classical torque applied to a rigid body. An ensemble of randomly oriented molecules will feel the polarity of the field, such that the librations of the molecule become restricted to a fixed angular range in θ, the angle between the molecular axis and the field vector.

In the "long" pulse limit, for which the pulse duration is much longer than the rotational period, $t_p \gg \tau_{rot} (\equiv \pi\hbar/B)$, the field appears static to the molecule and the interaction is adiabatic [146]. In the short pulse limit, for which the pulse duration is shorter than the rotational period of the molecule, $t_p < \tau_{rot}$, a "kick" of angular momentum is transferred to the system. Under such conditions, the interaction is nonadiabatic; the angular momentum of the system is not conserved and rotational transitions take place. A broad wave packet—or a coherent superposition of rotational levels— is formed in angular momentum space, such that the system is spatially well-aligned about the polarization direction [50, 53, 146, 147].

As discussed in Section 2.3.3, using moderate laser intensities should not ionize or dissociate the molecule. Furthermore, use of linearly polarized laser field implies that $M\hbar$, the projection of J on the laser polarization (space-fixed) axis, will remain constant, $\Delta M = 0$ (see Figure 2.8). As mentioned previously, only the electronic angular

momentum, composed of orbital (L) and spin (S) angular momentum, projects angular momentum onto the body-fixed z axis since all nuclear rotational angular momenta of the rigid rotor are normal to the molecular axis. Next, we will examine the wave packet dynamics of the linear rigid rotor system.

Solutions to the time-dependent Schrödinger equation: rotational wave packets

The time-dependent Schrödinger equation (Eq. (2.105)) for the rigid rotor in the presence of an external laser field is given as,

$$i\hbar\frac{\partial\Psi(t)}{\partial t} = (\hat{\mathbf{H}}_{rr} + \hat{\mathbf{V}}^{ext}(t))\Psi(t), \tag{2.221}$$

where the Hamiltonian for a rigid rotor is defined

$$\hat{\mathbf{H}}_{rr} = B\hat{\mathbf{J}}^2. \tag{2.222}$$

B is the rotational constant in the equilibrium geometry and $\hat{\mathbf{J}}^2$ is the total angular momentum operator squared. The time-dependent potential energy is given in the electric dipole approximation as

$$\hat{\mathbf{V}}^{ext}(t) = -\vec{\boldsymbol{\mu}}_0 \cdot \vec{E}(t) \tag{2.223}$$

where $\vec{\boldsymbol{\mu}}_0$ is the permanent electric dipole moment at the equilibrium geometry of the molecule. The electric field describing the HCP, $\vec{E}(t)$, is given as

$$\vec{E}(t) = \vec{\varepsilon}E_0\cos(\omega\, t + \varphi)\cdot s(t), \tag{2.224}$$

where E_0 is the field strength and $\vec{\varepsilon}$ is a unit vector along the polarization direction which, following convention, is the space-fixed Z axis, *i.e.* $\vec{\varepsilon}$ from Eq. (2.224) is $\vec{\varepsilon}_Z$. The phase is set to zero, $\varphi = 0$, for simplicity. One should note that the electric field given here differs slightly from the expression given in Eq. (2.134), namely cosine is used here instead of sine. (Of course, since $\cos x = -\sin(x - \pi/2)$, these expressions are related through a simple phase factor.)

In the nonresonant case, electronic and vibrational excitations do not occur; this condition implies that the carrier frequency, ω, be an off-resonant IR frequency, such that the molecule remains in the electronic ground state and avoids vibrational transitions. The envelope function, $s(t)$, that describes the HCP is chosen in this case to be a Gaussian function centered at time $t = t_0$:

$$s(t) = e^{-(t-t_0)^2/\sigma^2}. \tag{2.225}$$

The width of $s(t)$ at half the maximum height is given by $2\sigma\sqrt{\ln 2}$ (see Eq. (2.136)). The pulse duration σ is chosen such that it includes one half-cycle of the oscillating laser field. The interaction of the field with the dipole moment of the molecule can give rise to two interactions, a permanent dipole interaction and an induced dipole (polarizability) interaction. However, the nature of these interactions is controversial and still being debated by experts in the field [39, 148].

Herschbach and Friedrich write the interaction Hamiltonian for a cw laser as [39, 149],

$$\hat{\mathbf{V}}^{ext}(t) = -\vec{\boldsymbol{\mu}}_0 \cdot \vec{E}(t) = -\mu_0\, E(t) \cos\,\theta - \frac{1}{4}\boldsymbol{\alpha}^{\text{space}} {E_0}^2 \cos^2\,\theta, \tag{2.226}$$

where μ_0 is the permanent dipole moment and $\boldsymbol{\alpha}^{\text{space}}$ is the polarizability tensor in the space-fixed frame,

$$\boldsymbol{\alpha}^{\text{space}} = \begin{pmatrix} \alpha_{XX} & \alpha_{XY} & \alpha_{XZ} \\ \alpha_{YX} & \alpha_{YY} & \alpha_{YZ} \\ \alpha_{ZX} & \alpha_{ZY} & \alpha_{ZZ} \end{pmatrix}. \tag{2.227}$$

For nonresonant frequencies much greater than the reciprocal of the laser pulse duration, $\omega \gg \sigma^{-1}$, averaging over the pulse width σ quenches the dipole interaction—the mean value of $\mu_0\, E(t)$ averages to zero—and converts the second part of Eq. (2.226) to ${E_0}^2/2$ [39]. One should note that the $\cos^2\,\theta$ nature of the polarizability interaction enhances *alignment* rather than orientation. On the other hand, the dipole-field interaction scales according to $E(t)\cos\,\theta$ and thus contributes to molecular orientation.

According to Seideman, at far-off-resonance frequencies, first-order absorption processes can be neglected, and the induced dipole (polarizability) interaction is the leading term [148]. For pulsed laser fields, the polarizability-field interaction behaves as $[E_0 s(t)]^2 \cos^2\,\theta$, *i.e.* the polarization interaction depends on the pulse envelope $s(t)$ and not on the rapid oscillations of the laser field under the envelope. However, in the special case of a virtually unipolar half-cycle laser pulse at moderate to strong field strengths (10^{10} W/cm^2 - 10^{12} W/cm^2), the dipole coupling is the leading term and no polarizability interaction need be considered [145], *i.e.*:

$$\hat{\mathbf{V}}^{ext}(t) = -\vec{\boldsymbol{\mu}}_0 \cdot \vec{E}(t) = -\mu_0\, E(t) \cos\,\theta. \tag{2.228}$$

In the subsequent rotational wave packet dynamics simulations, we will use the interaction Hamiltonian from Eq. (2.228).

The wave function $|\Psi(t)\rangle$ can be expanded in a complete set of stationary eigenstates,

$$|\Psi(t)\rangle = \sum_{J\,\Omega\,M} C^{J\,\Omega\,M}(t) |J\,\Omega\,M\rangle e^{-iE_J t/\hbar}, \tag{2.229}$$

where $C^{J\,\Omega\,M}(t)$ are the time-dependent expansion coefficients and $e^{-iE_J t/\hbar}$ are time-dependent phase factors. The wave function $|J\,\Omega\,M\rangle$ is given in Eq. (2.220). Substitution of Eqs. (2.228) and (2.229) into the time-dependent Schrödinger equation (Eq. (2.221)) yields a set of coupled equations for the expansion coefficients:

$$i\hbar\dot{C}^{J\,\Omega\,M}(t) = \sum_{J'} C^{J'\,\Omega\,M}(t) \cdot \langle J\,\Omega\,M|-\vec{\boldsymbol{\mu}}_0 \cdot \vec{E}(t)|J'\,\Omega\,M\rangle e^{\frac{i}{\hbar}\Delta E_{JJ'}t}. \tag{2.230}$$

In Eq. (2.230), both M and Ω are conserved. $\Delta M = 0$ since the laser field is linearly Z-polarized, and $\Delta\Omega = 0$ since the electronic state of the molecule does not change. The values $\Delta E_{J\,J'}$ are the spacings between the rigid rotor rotational energies,

$$\Delta E_{JJ'} = E_J - E_{J'} = B\left[J(J+1) - J'(J'+1)\right]. \tag{2.231}$$

The interaction Hamiltonian is

$$\langle J\,\Omega\,M|-\vec{\boldsymbol{\mu}} \cdot \vec{E}(t)|J'\,\Omega\,M\rangle = -\mu_0\,E(t) \cdot W_{\mathrm{dip}}(J\,\Omega\,M|J'\,\Omega\,M)$$

where the integral over the Euler angles for the dipole interaction is

$$W_{\mathrm{dip}}(J\,\Omega\,M|J'\,\Omega'\,M') = \langle J\,\Omega\,M|\cos\,\theta|J'\,\Omega\,M\rangle. \tag{2.232}$$

The matrix elements in Eq. (2.232) can be evaluated using $3-J$ symbols, analagously to the integral over three rotation matrices in Eq. (2.219), where $\cos\,\theta$ is just the rotation matrix $D^1_{00}(\phi,\theta,0)$:

$$\begin{aligned}\langle J\Omega\,M|\cos\,\theta|J'\Omega M\rangle \;=\; & (-1)^{\Omega+M}\sqrt{(2J+1)(2J'+1)} \\ & \times \begin{pmatrix} J & 1 & J' \\ M & 0 & -M \end{pmatrix} \begin{pmatrix} J & 1 & J' \\ \Omega & 0 & -\Omega \end{pmatrix}.\end{aligned} \tag{2.233}$$

Starting with a pure rotational state $|J_i\,\Omega_i\,M_i\rangle$ (zero temperature limit) at $t = 0$, the time-dependent expansion coefficients can be expressed as,

$$C^{J\,\Omega\,M}(t=0) = \delta_{JJ_i}\delta_{\Omega\Omega_i}\delta_{MM_i}. \tag{2.234}$$

Quantifying orientation and alignment

Having discussed the tools for analyzing rotational wave packets, we can now return to the goal of orienting an ensemble of molecules using a linearly polarized, HCP. One quantitative measure of orientation is the expectation value $\langle J\,\Omega\,M|\cos\,\theta|J\,\Omega\,M\rangle \equiv \langle\cos\,\theta\rangle$ where θ is the angle between the z molecular axis and the Z space-fixed axis. In the case of a rigid rotor with non-zero spin and electronic orbital angular momentum, the orientation cosine $\langle\cos\,\theta\rangle$ can be evaluated using $3-J$ symbols with the following expression [150],

$$\langle\cos\,\theta\rangle = \sum_{JJ'} C^{J\Omega M} C^{J'\Omega M^*} \langle J\Omega\,M|\cos\,\theta|J'\Omega' M'\rangle e^{\frac{i}{\hbar}\Delta E_{JJ'}t} \tag{2.235}$$

The matrix elements $\langle J\Omega\, M|\cos\theta|J'\Omega' M'\rangle$ vanish for $M \neq M'$ and $\Omega \neq \Omega'$. The $3-J$ symbols (discussed in Section 2.4.3) represent Clebsch-Gordan coefficients.

Typically, a rotationally cooled molecular beam consists of a thermal average of rotational levels such that an isotropic distribution of magnetic states, $-J_i \leq M_i \leq J_i$, exists, and averaging must be performed over the initial distribution of M states [53]. The calculation of orientation and alignment observables must therefore include a Boltzmann weighting, or a thermal average over rotational states:

$$\langle\cos\theta\rangle_T(t) = {Q_{\rm rot}}^{-1} \sum_{J_i}^{J_{\rm max}} w_{J_i}(T) \sum_{M_i=-J_i}^{J_i} \langle\cos\theta\rangle_{J_i,M_i}(t). \tag{2.236}$$

where $w_J(T)=\exp(-E_J/k_BT)$, k_B is the Boltzmann constant, T is the temperature, and $Q_{\rm rot}$ is the rotational partitional function that runs from J_i to $J_{\rm max}$:

$$Q_{\rm rot} = \sum_{J_i}^{J_{\rm max}} (2J+1)\exp\left[\frac{-BJ(J+1)}{k_BT}\right]. \tag{2.237}$$

For higher temperatures, the thermally averaged rotational population contains a broader spread of J and M states than does a sample that is cooled to almost $T = 0$ K. This broader distribution in angular space leads to a diminished observed orientation (and alignment), as compared to the 0 K case. In other words, to achieve the same degree of orientation as in the 0 K case, the field would need to apply more "torque" to the system. The same reasoning applies to heavier molecules: more J levels are initially populated than are for lighter molecules at comparable temperatures, so these systems require more time to respond to the field. Nonetheless, a smaller rotational constant implies that rotational energy levels are more closely spaced and that higher angular momenta are accessed by the field at the same intensity, so that these competing effects lead to qualitatively similar results.

Let us now conclude with a discussion of one way in which orientation, or $\langle\cos\theta\rangle$, is measured experimentally. In the case of laser-induced orientation, a short ($t_p < \tau_{rot}$) orientation pulse is applied that creates a superposition of rotational eigenstates. Next, an intense femtosecond laser probes the sample by creating ions via Coulomb explosion, and a static field projects the ions onto the position-sensitive detector. Finally, $\langle\cos\theta\rangle$ can be measured, where θ is just the angle between the Z polarization axis of the laser and the projection of the ion velocity on the detector plane. This quantity is then a measure of the average orientation of the ensemble of molecules [47, 55].